

**Fresh Produce Spatial Price Equilibrium on General Networks:
Capturing Commodity Quality Deterioration
Through Endogenous Transportation Time Delay Functions with Capacities**

Anna Nagurney* and Samirasadat Samadi

Department of Operations and Information Management

Isenberg School of Management

University of Massachusetts

Amherst, Massachusetts 01003

Deniz Besik

Robins School of Business

University of Richmond

Richmond, Virginia 23173

European Journal of Operational Research (2026), **334(1)**, pp 249-270.

Abstract: Fresh produce is vital to global food security but is highly vulnerable to transportation delays and capacity disruptions, as in critical links such as the Panama Canal. This paper develops a commodity fresh produce trade equilibrium model under quality deterioration on a general network, allowing for multiple transportation links on a path between supply and demand markets. We extend the Bureau of Public Roads (BPR) congestion function to endogenize time delay as a function of all commodity shipments on a link. By embedding link upper bounds in time delay functions, we capture how upper bounds impact transportation times and fresh produce quality. The spatial price equilibrium conditions are formulated as a variational inequality problem. We also propose commodity quality trade network performance measures, supply-based, demand-based, and network-based, that can be applied for an individual commodity or across all commodities. We apply the model to bananas, a globally popular and nutritious fruit, and its trade from Ecuador and Costa Rica to the European Union, the United States, and Russia, focusing on drought-driven congestion at the Panama Canal. Numerical examples, whose solutions are computed using the modified projection method, show that reductions in transportation link upper bounds and increased free-flow transportation times significantly lower banana shipments, degrade their quality, and shift prices at both supply and demand markets. We include benchmark comparisons with linear congestion and no-congestion specifications to explicitly quantify how nonlinear congestion modeling alters equilibrium flows, prices, transportation times, and quality deterioration. These comparisons reveal that linear and no-congestion specifications can misrepresent congestion effects, particularly when flows operate at moderate-to-high utilization levels. The results align closely with real-world data on banana prices, transportation costs, and export volumes, reinforcing the model's practical relevance. Our model provides decision-makers with essential insights on the impacts of congestion and increasing transportation times on fresh produce trade and its quality, along with the performance of the trade network.

Keywords: networks, equilibrium, transportation, variational inequalities, fresh produce quality

* corresponding author: nagurney@isenberg.umass.edu

1. Introduction

Fresh produce, in the form of fresh fruits and vegetables, is essential for the health and well-being of societies. Fresh fruits and vegetables are produced by farmers in different parts of the globe, and then transported to demand markets for purchase by consumers. Such fresh produce trade networks help to support food security and provide consumers with nutrition. The global revenue in 2022 from fresh vegetables was expected to be 691.20 billion US dollars and 622.80 billion US dollars for fresh fruit with the expected volume growth for 2023 being 3.2% and 2.9%, respectively (International Fresh Produce Association (2023)). Furthermore, although the World Health Organization recommends 400 grams of fruits and vegetables per day per person, world production is at 390 grams per person per day, with world consumption at only 267 per person per day.

Fresh produce is perishable, and, hence, even under the best conditions, its quality deteriorates over time (see Yu and Nagurney (2013)). Major challenges now associated with transportation include, among others: congestion on roads and at seaports, reduced capacity of major links such as the Panama Canal, because of a drought, as well as of the Red Sea and the Suez Canal, because of man-made attacks, plus maritime route capacity reductions on the Black Sea due to Russia's full-scale invasion of Ukraine and Russia's pulling out of the Black Sea Grain Initiative (cf. Nagurney et al. (2023, 2024a,b)). Hence, the quantification of fresh produce quality as it makes its way from supply markets to demand markets on transportation networks, along with the volumes of such trade, and the prices that consumers pay, are all of relevance.

Issues of insufficient capacity on transportation links, which can also lead to congestion, have resulted in products, including fresh produce, being rerouted with costly time delays and accompanying economic losses. According to Ramirez (2023), the Panama Canal Authority decreased the number of daily cargo ship slots from 32 to 24 at the beginning of November 2023, with the number expected to drop to 18 by February 2024. Freight service providers that focus on refrigerated products were considering traveling around South America to transport harvests of various fruits, including Chilean cherries, which would result in a week's delay in the arrival of the fruit.

On the other side of the globe, according to the United States Department of Agriculture Foreign Agricultural Service (2024), the attacks by Houthi rebels in Yemen, since mid December 2023, on the Red Sea and the Suez Canal, considered to be among the world's busiest shipping routes, have disrupted global trade, including the export of Egyptian citrus fruit. Multiple container shipping companies are diverting their ships to a much longer route around the Cape of Good Hope, which has increased the transportation time by approximately two weeks from Europe to Asia (Lin (2025)). This can result in the fresh produce rotting.

Bananas play a significant role in global trade, being one of the most widely consumed and traded fruits and a crucial agricultural commodity, as a key source of nutrition for millions of people (Food and Agriculture Organization of the United Nations (2025)). As a perishable commodity, bananas are highly sensitive to transportation disruptions and delays, such as those caused by environmental

and geopolitical factors. In fact, 82% of the banana exports from Ecuador, the largest banana exporter, pass through the Panama Canal (FreshPlaza (2025)), making any drought there, with the resulting reduction in capacity particularly problematic (FreshFruitPortal.com (2024)). The recent persistent drought in the Panama Canal has led ships carrying bananas to wait longer or to reroute, increasing shipping times and costs. According to ProducePay (2023), bananas may be the most heavily impacted fruit, given the extensive use of the Panama Canal for their exports. Consequently, banana exporters and importers face difficulties in meeting the global demand while preserving quality at reasonable prices.

Issues associated with transportation and impacts on supply chains were already exacerbated in the COVID-19 pandemic. Liu, Wang, and Chen (2023) note that, since the beginning of this pandemic, ports globally have been experiencing increasing congestion, with the media reporting in 2021 that more than 300 container ships around the globe queued up at ports waiting to be unloaded. This level was double the congestion experienced at the beginning of that year, with some ships at the ports of Los Angeles and Long Beach waiting more than twelve days to unload their cargo.

It is important to recognize that the transportation of fresh produce can involve different modes of transportation, such as trucks, railways, barges, ships, and even air freight, or a combination thereof (cf. Millard (2019)). The type of transport mode(s) used will depend on geographical distance, urgency of deliveries, financial budgets, etc., and each link in the transportation network plays a role in reducing fresh produce quality deterioration.

While exogenous disruptions such as droughts or bottlenecks reduce the available transportation capacity, the resulting congestion effects are endogenous to shipment volumes. In other words, as more commodities compete for limited capacity on a route, transportation times rise nonlinearly rather than proportionally. To capture this relationship, we extend the classical Bureau of Public Roads (BPR) function, which models how transportation time increases as the ratio of flow to capacity grows. Most existing trade and supply chain network models, including those addressing perishability, assume transportation time is fixed or linearly related to flow. The BPR function has been widely used in transportation and logistics to represent congestion effects (see Kim and Mahmassani (1987), Sanders et al. (2007)), where even modest increases in flow under near-capacity conditions can lead to disproportionately large increases in transportation time. This nonlinear behavior is analogous to queuing systems, where waiting times escalate sharply as system utilization approaches capacity, producing similar congestion dynamics. Capturing this nonlinearity is particularly important for perishable commodities, since longer transportation times directly translate into quality deterioration, altered demand prices, and equilibrium flows.

In this paper, we contribute to the literature by constructing a novel commodity trade network equilibrium model for fresh produce that captures quality deterioration and that allows for multiple transportation routes/paths connecting each pair of supply and demand markets. Each route/path can consist of one or more links, with a link corresponding to a specific mode of transportation. The supply and the demand markets can be in the same or in different countries. Another distinguishing

feature of the network model is that the transportation time on a link is quantified through an extension of the classical Bureau of Public Roads cost function (see Special Report 209: Highway Capacity Manual (1985)), which includes capacities on links endogenously. The time, along with relevant parameters, influences the quality of the fresh produce as it is transported on transportation links from a supply market to a demand market. To illustrate the model and its implications, we provide both simple examples (a single commodity one and a two commodity one) and then algorithmically solved numerical examples using bananas as a representative perishable product. The examples examine how equilibrium flows, prices, transportation times, and quality respond to changes in transportation link upper bounds and free-flow transportation times. In addition, the numerical analysis includes a comparison of our nonlinear congestion function formulation with that of linear congestion and no-congestion specifications, highlighting how endogenous congestion and capacity affect equilibrium outcomes relative to models with fixed or linear transportation times.

2. Literature Review, Our Contributions, and Organization of This Paper

In this section, we provide a review of the literature in Subsection 2.1, emphasizing the most relevant papers related to our new model. We also note the specific enhancements associated with the new model in Subsection 2.2, and highlight how the remainder of the paper is organized in Subsection 2.3.

2.1 Literature Review

In order to provide the proper context for our contributions, we present the literature review, focusing on the necessary background and foundational papers. The literature review is divided into fresh produce commodity perishability and generalized networks, with the use of arc multipliers, supply chain network models and spatial price equilibrium ones with fresh produce quality deterioration, and commodity trade network models with capacities.

2.1.1 Fresh Produce Commodity Perishability and Generalized Networks

In terms of commodity perishability and spatial price equilibrium models, the majority of the literature has made use of generalized networks in which there are arc multipliers. In particular, Thore (1986) was the first to utilize arc multipliers for perishability in the framework of spatial price equilibrium problems, but assumed separable functions. Nagurney and Aronson (1989) developed a dynamic spatial price equilibrium model with gains and losses using variational inequality theory. Yu and Nagurney (2013) proposed an oligopolistic fresh produce supply chain network equilibrium model with arc multipliers using game theory. More recently, Nagurney and Besik (2022) developed a commodity spatial price network equilibrium model in which the arc multipliers are flow-dependent but the authors assumed a single route between each pair of supply and demand markets.

2.1.2 Supply Chain Network Models and Spatial Price Equilibrium Models with Fresh Produce Quality Deterioration

Besik and Nagurney (2017) were the first to make use of fresh produce quality deterioration formulae based on food science in their supply chain network model of competitive farmers' markets in an oligopolistic setting. A further extension was then made in the paper by Besik, Nagurney, and Dutta (2023). However, the authors assumed that the time on a transportation (or storage) link was known and fixed and was not influenced by congestion. The models were all imperfectly competitive models, whereas our new model is a perfectly competitive one, with classical such works being the spatial price equilibrium models of Samuelson (1952) and Takayama and Judge (1964, 1971). Our new model, nevertheless, makes use of the theory of variational inequalities for the formulation, analysis, and computation of the equilibrium supply price, commodity shipment, and demand price pattern. In addition, here we construct a price and quantity model, whereas the previously noted models were all in quantity variables exclusively. Furthermore, our new model extends the model of Besik and Nagurney (2025) in multiple, significant ways, which we enumerate in Subsection 2.2. Additional background on spatial price equilibrium models using a variational inequality formalism can be found in the papers by Florian and Los (1982), Dafermos and Nagurney (1984), and in the book by Nagurney (1999). Outside spatial price equilibrium models, de Keizer et al. (2017) developed a mixed-integer linear programming logistics network model for perishable products that explicitly incorporated heterogeneous quality decay along transportation, storage, and processing activities, and demonstrated how quality deterioration can affect network structure and flow patterns. Fresh produce commodities, with their associated trade networks, are distinct from other types of commodities due to their perishable nature. As biological products, fruits and vegetables continuously deteriorate in quality over time, even under optimal storage and transportation conditions (cf. Besik and Nagurney (2017)). This perishability poses unique challenges for managing fresh produce trade networks, particularly as congestion and delays along transportation routes can further influence shipment volumes, market prices, and the ultimate quality of the products that reach demand markets.

2.1.3 Commodity Trade Network Models with Capacities

Nagurney et al. (2023) introduced an international commodity trade network equilibrium model with exchange rates and allowed for multiple paths between supply and demand market pairs. The authors also considered upper bounds on commodity shipments but they were commodity-specific and not link-specific. Furthermore, that model did not consider quality of commodities. Nagurney et al. (2024a), in turn, developed a commodity trade network equilibrium model with upper bounds at supply markets and on transportation routes across commodities but each route consisted of a single link. Nagurney et al. (2024b), building upon the work of Nagurney et al. (2024a), considered multiple possible disaster scenarios that would impact such upper bounds. In addition, trade network performance measures were introduced. Both of these papers, however, did not consider quality deterioration, as we do here. Hassani et al. (2025) built a multiperiod trade network equilibrium model with capacities on links, including storage links, but the model did not

include quality deterioration of fresh produce and was in quantity variables and not in price and quantity variables as is the model in this paper. Moreover, transportation time on links was not made explicit in the above noted papers, as we do in our new model in this paper. In particular, here we extend congestion functions to multiple commodities and they endogeneously include link capacities. These functions capture time delay and, in turn, affect the quality deterioration of the fresh produce according to given decay functions. Birge et al. (2022) analyzed single commodity spatial trade networks with separable functions and fixed transportation costs with capacities on links and applications to energy.

2.2 Our Contributions

The commodity trade network equilibrium model in this paper is most closely influenced by the fresh produce trade model with quality deterioration developed by Besik and Nagurney (2025). However, the model in this paper differs from the earlier one in significant ways. Below we delineate the novel contributions in this paper.

1. Here we allow for each path/route connecting a pair of supply and demand markets to consist of one or more links. The model of Besik and Nagurney (2025) did allow for multiple routes connecting each pair of supply and demand markets but each route consisted of a single link. Fresh produce transportation can involve trucking, followed by maritime shipping or air freight, followed by additional trucking or even railways, and, therefore, having the flexibility of routes consisting of multiple links is relevant for practice, since bottlenecks and time delays may arise on one or more links.

2. In this paper, the congestion (time delay) functions can have a nonlinear dependence on commodity shipments, whereas in Besik and Nagurney (2025) the influence on congestion was assumed to be linear. Furthermore, in our new congestion functions, we include the influence of all the commodities that may be using a particular link. Hence, this paper advances prior work (Besik and Nagurney (2025)) by explicitly endogenizing transportation time on each link as a nonlinear function of the total shipment volume and link capacity. Specifically, we extend the classical Bureau of Public Roads (BPR) function, widely used in transportation and congestion modeling, to the multiple commodity trade setting. This formulation allows transportation time to respond endogenously to congestion, thereby linking flow-dependent delays to perishable quality deterioration within the equilibrium framework. In contrast, prior models assumed linear or exogenous transportation times, which can misrepresent the magnitude and spatial distribution of delays under congestion (see Kim and Mahmassani (1987), Sanders et al. (2007)). The proposed approach provides a more realistic and policy-relevant representation of how congestion propagates through the trade network and affects both commodity quality and equilibrium prices. To further illustrate the implications of this modeling extension, several of the numerical examples reveal how equilibrium outcomes differ under nonlinear congestion, linear congestion, and fixed transportation time specifications. This comparison highlights how endogenizing congestion and capacity affects flows, prices, transportation times, and the final commodity quality relative to more simplified congestion assumptions.

3. The model in this paper is in price and quantity variables, whereas the earlier model was in quantity variables, but the initial quality of each commodity was a variable at each supply market, with associated costs. Here, in contrast, we assume a fixed and known initial quality level for each commodity at each supply market. This does have the advantage of one not needing to estimate opportunity cost functions. Having prices as explicit variables allows for transparent analysis of price transmission along the trade network. Additionally, the model allows demand prices to vary by transportation route. This captures a key characteristic of perishable commodities since consumers value such commodities differently depending on the quality of the commodities that they receive, and quality varies with transportation time. Lastly, modeling prices as explicit variables facilitates comparison with observed market prices, since equilibrium prices are direct outputs of the model, thereby enhancing its empirical relevance.

4. The upper bounds in Besik and Nagurney (2025) were imposed on commodity shipments individually on each route, which, as noted earlier, consisted of a single link. In the model in this paper, in contrast, upper bounds are endogenous to the time delay functions and, therefore, the influence of upper bounds reduction (or enhancement) on quality deterioration of fresh produce can be more directly quantified, upon model solution. Both commodity trade network equilibrium models for fresh produce, nevertheless, utilize variational inequality theory for the formulation of the equilibrium conditions, the accompanying theoretical qualitative analysis, and the algorithm development.

5. In this paper, we also propose commodity quality trade network performance measures. The measures are supply-based, demand-based, as well as network-based and on individual commodity levels as well as across all commodities. Such measures are novel and allow decision-makers to assess which supply markets are performing well from a quality standpoint; the same for the demand markets, and the trade network, as a whole. Nagurney et al. (2024b) provided trade network performance measures under disaster scenarios but did not capture commodity quality as we do in this paper.

Our paper, hence, integrates BPR-type time delay functions, capacities, and quality deterioration in a perishable trade network, evaluated with performance measures.

2.3 Organization of This Paper

The paper is organized as follows. In addition to the above Introduction and the Literature Review and Our Contributions subsections, in Section 3, we construct the model, provide the equilibrium conditions, and give their interpretation. We then establish the variational inequality formulation and present two illustrative examples, with the first one focusing on bananas, and the second one on bananas and watermelons. We follow with some qualitative results for the new model. In Section 4, the commodity quality trade network performance measures are introduced. In Section 5, we construct a series of numerical examples, focusing on the banana trade, that are solved algorithmically, and that reflect real-world scenarios. Section 6 summarizes the results and provides suggestions for future research.

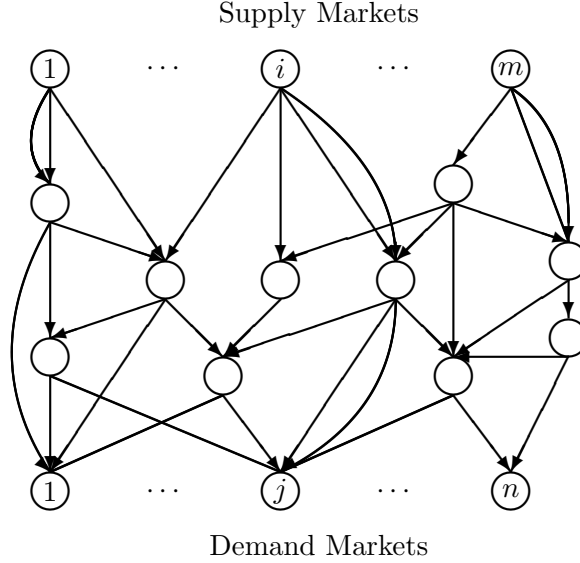


Figure 1: A Trade Network Topology

3. The Commodity Fresh Produce Trade Equilibrium Model on a General Network

We now construct the commodity fresh produce trade equilibrium model with time delays on a general network. There are m supply markets, with a typical supply market denoted by i , and n demand markets, with a typical demand market denoted by j . The supply and demand markets can be in the same region of a country or in different regions of different countries. They are spatially separated. The supply markets are involved in the production of K commodities, with a typical commodity denoted by k , and the commodities are consumed at the demand markets. The commodity formulation reflects realistic trade conditions in which several agricultural products are shipped simultaneously through shared transportation links, leading to possible congestion and capacity interactions across commodities. Underlying the supply markets and demand markets is a network topology consisting of a graph $G = [N, L]$, where N is the set of nodes consisting of: the supply market origin nodes, the demand market destination nodes, intermediate nodes for transshipment, etc., and L is the set of directed links. An example of a trade network topology is depicted in Figure 1. There are n_P paths in the network, with P denoting the set of paths, and n_L links. We denote a typical link by a and a typical path, originating at a supply market node and terminating at a demand market node, by p .

3.1 Preliminaries and Extension of Time Delay Functions

Since we are dealing with fresh produce, such as fruits and vegetables, which are perishable commodities, we need to recall some concepts from food science in terms of commodity quality deterioration. Specifically, according to Taoukis and Labuza (1989), the quality deterioration rate is affected by factors such as the gas composition, the relative humidity, and the temperature, with Labuza (1984) providing the differential equation for quality, q , which reflects a particular food

attribute over time, given by:

$$\frac{\partial q}{\partial t} = -\kappa q^b = -Ae^{\left(\frac{-E_A}{RT}\right)} q^b. \quad (1)$$

In the differential equation above, κ denotes the reaction rate, according to the Arrhenius formula: $-Ae^{\left(\frac{-E_A}{RT}\right)}$, with A being the pre-exponential constant, T being the temperature, and E_A denoting the activation energy. R is the universal gas constant (cf. Arrhenius (1889)) and b denotes the reaction order. In this paper, we consider $b = 0$; that is, zero-order quality decay, which is characteristic of such popular fresh produce items as: bananas, strawberries, watermelon, and broccoli (cf. Besik and Nagurney (2017, 2025)).

Hence, w.l.o.g., given an initial quality, q^0 (see also Tijskens and Polderdisk (1996)), we have that:

$$q = q^0 - \kappa t. \quad (2)$$

We now adapt the above to our model on a general trade network and also expand on the time delay functions associated with the links.

We recall that Besik and Nagurney (2017) constructed quality formulae on paths for fresh produce but in an oligopolistic setting and considered a single commodity. We let β_a^k denote the quality decay incurred by commodity k on link a such that

$$\beta_a^k = -\kappa_a^k t_a, \quad \forall a \in L, \quad (3)$$

where

$$\kappa_a^k = Ae^{\left(\frac{-E_a}{RT_a^k}\right)}, \quad \forall k, \forall a, \quad (4)$$

and t_a is the time on link a .

Observe that, according to (3), the time on a link is assumed to be the same for all commodities. This is so because different commodities may be transported on the same links and add to the time delay as we, subsequently, quantify in the expansion of the classical Bureau of Public Roads (BPR) formula (cf. Traffic Assignment Manual (1964)).

Note that, according to (4), the temperature of commodities on a link may differ since we have T_a^k , for all k and for all a . We group all the commodity link temperatures into the vector $T \in R^{Kn_L}$.

Hence, the quality of commodity k on path p , q_p^k , with the path p originating at a supply market i , takes the form:

$$q_p^k = q_i^{0k} + \sum_{a \in p} \beta_a^k, \quad \forall k, \forall p \in P^i, \forall i, \quad (5)$$

where q_i^{0k} denotes the initial quality of commodity k produced at supply market i and P^i denotes all the paths emanating from supply market node i . We also let P_j denote the set of all paths originating at the supply markets and terminating at demand market node j with P_j^i denoting the set of all paths joining supply market i with demand market j .

We now expand upon the time t_a on a link $a \in L$. In previous supply chain based models for fresh produce (cf. Yu and Nagurney (2013), Besik and Nagurney (2017), and Besik, Nagurney, and Dutta (2023)) the time on a link was assumed to be known and fixed. Here, in contrast, the time can be commodity flow-dependent and also dependent on the upper bound associated with the link, with u_a denoting the upper bound on link a , for all $a \in L$. We let f_a^k denote the flow of commodity k on link a , for all commodities k and all links a . In particular, we make use of an expansion of the Bureau of Public Road (BPR) functions as follows:

$$t_a = t_a^0 \left(1 + \alpha_a \left(\frac{\sum_{k=1}^K \eta_a^k f_a^k}{u_a} \right)^{\gamma_a} \right), \quad \forall a \in L, \quad (6)$$

where the η_a^k is a positive parameter for all k and for all a , and α_a is also a positive parameter for all a since we assume congestion effects. The structure of (6) is inspired by the work of Kim and Mahmassani (1987), who noted the Special Report 209: Highway Capacity Manual (1985), in extending the classical BPR function to multiple modes of transportation. In our model, a link corresponds to a mode of transportation but the flows are commodity-specific, since we are dealing with freight and not with passenger transportation.

As can be seen from (6), if the upper bound on a link is high, then the impact of the volume of commodity flow on the link is lower, and the transportation time is lower. If, on the other hand, the upper bound is lower, then the transportation time would be higher. Furthermore, the value of the exponent γ_a , which is nonnegative, as is α_a for all links $a \in L$, represents how the transportation time on a link is affected by the commodity flow on the link. In classical BPR functions, the exponent would, typically, be 4 and the only flow would be that link's flow. Here, we capture the effects of commodity transport on links. We group all the link times into the vector $t \in R^{n_L}$.

Note that t_a^0 in (6) can be interpreted as the “free flow” transportation time; that is, when $\sum_{k=1}^K \eta_a^k f_a^k = 0$. Here, since we are dealing with agricultural commodities, and their units are, typically, tons, we can do such a summation as $\sum_{k=1}^K \eta_a^k f_a^k$ (see, also, e.g., Nagurney et al. (2024a)). It is important to recognize that, in our model, links can correspond to different modes of transportation used for the shipment of agricultural products with possible modes of transportation being: rail, trucks, barges, ships, and even air freight. Furthermore, although BPR functions have focused on road transport, others have utilized adaptations of such functions to capture congestion in the case of maritime transportation (see Sanders, Verhaeghe, and Dekker (2007)). Yan (2016) adapted BPR functions to model containerized global maritime shipping delays in his thesis. Glauser (2021) also derived congestion functions using BPR constructs focusing on shipping through the Panama and Suez Canals in his thesis. Yamada et al. (2009), in their freight network design model, utilized BPR type functions to capture delay associated with multiple modes of transportation (road, rail, and sea). The International Transport Forum (2016) argued in its report that BPR functions are relevant to freight flows, including maritime shipments, in their international trade framework. However, none of these studies constructed a multiple commodity analogue of the BPR function as we have done in this paper. About 90% of the world's products are shipped via maritime transportation.

Hence, the quality of commodity k on path $p \in P^i$ takes the form:

$$q_p^k = q_i^{0k} - \sum_{a \in p} \kappa_a^k t_a^0 (1 + \alpha_a (\frac{\sum_{k=1}^K \eta_a^k f_a^k}{u_a})^{\gamma_a}), \quad \forall k, \forall p \in P^i. \quad (7)$$

We group all the commodity quality levels for all the paths into the vector $q \in R^{Kn_P}$.

3.2 Model Construction and Equilibrium Conditions

The fundamental notation for the model is given in Table 1. All vectors are column vectors. All costs and prices are in a common currency.

Table 1: Notation for the Fresh Produce Commodity Trade Network Equilibrium Model

Variables	Definition
x_p^k	the flow of commodity k on path p . We group the commodity path flows into the vector $x \in R_+^{Kn_P}$.
f_a^k	the flow of commodity k on link a . We group the commodity link flows into the vector $f \in R_+^{Kn_L}$.
π_i^k	the supply price of commodity k at supply market i . We group all the commodity supply market prices into the vector $\pi \in R^{Km}$.
ρ_p^k	the demand price of commodity k transported on path p . We group all the commodity demand market prices into the vector $\rho \in R^{Kn_P}$.
Functions	Definition
$c_a^k(f, t, T)$	the unit cost of transportation of commodity k on link a .
$C_p^k(x, t, T)$	the unit cost of transportation of commodity k on path p . We group all the path costs into the vector $C \in R^{Kn_P}$.
$s_i^k(\pi)$	the supply of commodity k at supply market i . We group all the supply functions into the vector $s(\pi) \in R^{Km}$.
$d_p^k(\rho, q)$	the demand for commodity k that has been transported on path p . We group all the demand functions into the vector $d(\rho, q) \in R^{Kn_P}$.

We now introduce the basic conservation of flow equations. The commodity path flows must be nonnegative, that is:

$$x_p^k \geq 0, \quad \forall k, \forall p \in P. \quad (8)$$

The commodity link flows are related to the commodity path flows thus:

$$f_a^k = \sum_{p \in P} x_p^k \delta_{ap}, \quad \forall k, \forall a \in L, \quad (9)$$

and, therefore, the commodity flow on a link is equal to the sum of flows of that commodity on paths that contain that link.

Furthermore, the unit transportation cost of a commodity on a path is equal to the sum of the

unit transportation costs for that commodity on the links that comprise the path; that is:

$$C_p^k(x, t, T) = \sum_{a \in L} c_a^k(f, t, T) \delta_{ap}, \quad \forall p \in P, \quad (10)$$

where $\delta_{ap} = 1$, if link a is contained in path p , and 0, otherwise.

In view of the conservation of flow equations (9), we may re-express the path quality levels (7) as:

$$q_p^k = q_i^{0k} - \sum_{a \in p} \kappa_a^k t_a^0 \left(1 + \alpha_a \left(\frac{\sum_{k=1}^K \eta_a^k \sum_{p \in P} x_p^k \delta_{ap}}{u_a} \right)^{\gamma_a} \right), \quad \forall k, \forall p \in P^i, \forall i. \quad (11)$$

In addition, in view of (11), we can define new demand price functions $\tilde{d}_p^k(\rho, x) \equiv d_p^k(\rho, q)$, for all k and for all p . This transformation allows us to formulate and solve the trade network equilibrium problem in supply price, demand price, and commodity path flow variables, and then to recover the quality levels of the commodities at the demand markets through the formulae (11). Also, in view of (7) and (9), we can define new unit path cost functions: $\tilde{C}_p^k(x, T) \equiv C_p^k(x, t, T)$, for all commodities k and all paths p .

We define the feasible set \mathcal{K} thus:

$$\mathcal{K} \equiv \{(x, \pi, \rho) \mid (x, \pi, \rho) \in R_+^{K(n_P+m+n_P)}\},$$

which is the nonnegative orthant and we state the governing commodity trade network equilibrium conditions below.

Definition 1: Commodity Fresh Produce Trade Network Equilibrium Under Quality Deterioration on a General Network with Time Delays

A commodity path flow, supply price, and demand price pattern $(x^*, \pi^*, \rho^*) \in \mathcal{K}$ is a fresh produce trade network equilibrium under quality deterioration on a general network with time delays, if the following conditions hold: For all commodities k ; $k = 1, \dots, K$, and for all paths p connecting pairs of supply and demand markets (i, j) ; $i = 1, \dots, m$ and $j = 1, \dots, n$:

$$\pi_i^{k*} + \tilde{C}_p^k(x^*, T) \begin{cases} = \rho_p^{k*}, & \text{if } x_p^{k*} > 0, \\ \geq \rho_p^{k*}, & \text{if } x_p^{k*} = 0; \end{cases} \quad (12)$$

for all commodities k and all supply markets i :

$$s_i^k(\pi^*) \begin{cases} = \sum_{p \in P^i} x_p^{k*}, & \text{if } \pi_i^{k*} > 0, \\ \geq \sum_{p \in P^i} x_p^{k*}, & \text{if } \pi_i^{k*} = 0, \end{cases} \quad (13)$$

plus, for all commodities k and for all paths p terminating at the demand markets:

$$\tilde{d}_p^k(\rho^*, x^*) \begin{cases} = x_p^{k*}, & \text{if } \rho_p^{k*} > 0, \\ \leq x_p^{k*}, & \text{if } \rho_p^{k*} = 0. \end{cases} \quad (14)$$

Equilibrium conditions (12) state that there will be a positive flow of a fresh produce commodity on a path, in equilibrium, if the supply price of the commodity at the supply market where it is produced plus the unit path cost of transporting the commodity on the path is equal to the price the consumers are willing to pay at the demand market. If, on the other hand, the above supply price plus the unit path transportation exceeds the price that the consumers are willing to pay, then the commodity flow on that path will be equal to zero.

Equilibrium conditions (13) state that the supply of a commodity produced at a supply market at the equilibrium is equal to the commodity shipments from the supply market to all the demand markets if the equilibrium commodity supply price is positive. On the other hand, if the equilibrium supply price is equal to zero, then there could be an excess supply of the commodity at the supply market.

Equilibrium conditions (14) state that for each commodity, if the equilibrium demand price at a demand market is positive, reflected by the demand for the commodity on a path (since different paths may result in different quality levels due to different time delays, etc.) then the demand is equal to the flow of the commodity on the path. If the demand price is zero, then the commodity flow on the path can exceed the demand.

We now derive the variational inequality formulation of the above equilibrium conditions in a Theorem.

Theorem 1: Variational Inequality Formulation of the Commodity Fresh Produce Trade Network Equilibrium Under Quality Deterioration on a General Network with Time Delays

A commodity path flow, supply price, and demand price pattern $(x^, \pi^*, \rho^*) \in \mathcal{K}$ is a fresh produce trade network equilibrium under quality deterioration on a general network with time delays, according to Definition 1, if and only if it satisfies the variational inequality problem:*

$$\begin{aligned}
& \sum_{k=1}^K \sum_{i=1}^m \sum_{j=1}^n \sum_{p \in P_j^i} \left[\pi_i^{k*} + \tilde{C}_p^k(x^*, T) - \rho_p^{k*} \right] \times \left[x_p^k - x_p^{k*} \right] \\
& + \sum_{k=1}^K \sum_{i=1}^m \left[s_i^k(\pi^*) - \sum_{p \in P^i} x_p^{k*} \right] \times \left[\pi_i^k - \pi_i^{k*} \right] \\
& + \sum_{k=1}^K \sum_{p \in P} \left[x_p^{k*} - \tilde{d}_p^k(\rho^*, x^*) \right] \times \left[\rho_p^k - \rho_p^{k*} \right] \geq 0, \quad \forall (x, \pi, \rho) \in \mathcal{K}.
\end{aligned} \tag{15}$$

Proof of Theorem 1: First, we establish necessity, that is, we show that if $(x^*, \pi^*, \rho^*) \in \mathcal{K}$ satisfies the network equilibrium conditions (12), (13), and (14) in Definition 1, then it also satisfies variational inequality (15). From the equilibrium conditions (12), for fixed k, i, j , and for a fixed

path $p \in P_j^i$; we know that:

$$\left[\pi_i^{k*} + \tilde{C}_p^k(x^*, T) - \rho_p^{k*} \right] \times \left[x_p^k - x_p^{k*} \right] \geq 0, \quad \forall x_p^k \geq 0, \quad (16)$$

since, if $x_p^{k*} > 0$, then the left-hand side of (16) preceding the multiplication sign is zero, so (16) holds. Also, if $x_p^{k*} = 0$, then the left-hand side expression, which precedes the multiplication sign, is nonnegative, and, since the path flows are nonnegative, $[x_p^k - x_p^{k*}] \geq 0$. The product of the two terms is also nonnegative and (16) holds. Since (16) is true for any k, i, j , and $p \in P_j^i$, summation of (16) over these indices yields:

$$\sum_{k=1}^K \sum_{i=1}^m \sum_{j=1}^n \sum_{p \in P_j^i} \left[\pi_i^{k*} + \tilde{C}_p^k(x^*, T) - \rho_p^{k*} \right] \times \left[x_p^k - x_p^{k*} \right] \geq 0, \quad \forall x \in R_+^{KnP}. \quad (17)$$

In addition, from equilibrium conditions (13), it follows that, for a fixed k, i :

$$\left[s_i^k(\pi^*) - \sum_{p \in P^i} x_p^{k*} \right] \times \left[\pi_i^k - \pi_i^{k*} \right] \geq 0, \quad \forall \pi_i^k \geq 0. \quad (18)$$

The summation of (18) over all k and i yields:

$$\sum_{k=1}^K \sum_{i=1}^m \left[s_i^k(\pi^*) - \sum_{p \in P^i} x_p^{k*} \right] \times \left[\pi_i^k - \pi_i^{k*} \right] \geq 0, \quad \forall \pi \in R^{Km} \geq 0. \quad (19)$$

Also, (14) implies that, if ρ_p^{k*} satisfies (14), then for a fixed k and for a fixed path $p \in P$:

$$\left[x_p^{k*} - \tilde{d}_p^k(\rho^*, x^*) \right] \times \left[\rho_p^k - \rho_p^{k*} \right] \geq 0, \quad \forall \rho_p^k \geq 0. \quad (20)$$

But inequality (20) holds for any k and p , so summation over all p and k yields:

$$\sum_{k=1}^K \sum_{p \in P} \left[x_p^{k*} - \tilde{d}_p^k(\rho^*, x^*) \right] \times \left[\rho_p^k - \rho_p^{k*} \right] \geq 0, \quad \forall \rho \in R^{KnP}. \quad (21)$$

Adding (17), (19), and (21) results in variational inequality (15). Thus, necessity has been established.

We now turn to establishing sufficiency; that is, we show that if $(x^*, \pi^*, \rho^*) \in \mathcal{K}$ satisfies variational inequality (15), then it also satisfies the spatial price equilibrium conditions (12) - (14).

Let $\pi_i^k = \pi_i^{k*}$, $\forall k, \forall i$; $\rho_p^k = \rho_p^{k*}$, $\forall k, \forall p$; and $x_p^k = x_p^{k*}$, $\forall k \neq \tilde{k}, \forall p \neq \tilde{p}$, with $\tilde{p} \in P_j^{\tilde{i}}$. Substitution of the resultants into (15), reduces the variational inequality (15) to:

$$\left[\pi_i^{\tilde{k}*} + \tilde{C}_{\tilde{p}}^{\tilde{k}}(x^*, T) - \rho_{\tilde{p}}^{\tilde{k}*} \right] \times \left[x_{\tilde{p}}^{\tilde{k}} - x_{\tilde{p}}^{\tilde{k}*} \right] \geq 0, \quad \forall x_{\tilde{p}}^{\tilde{k}} \geq 0, \quad (22)$$

from which the equilibrium conditions (12) hold.

By setting now $x_p^k = x_p^{k^*}$, $\forall k, \forall p$; and $\pi_i^k = \pi_i^{k^*}$, $\forall k, \forall i \neq \tilde{k}, \tilde{i}$ and substituting the resultant values into (15), yields:

$$\left[s_i^{\tilde{k}}(\pi^*) - \sum_{p \in P^{\tilde{i}}} x_p^{\tilde{k}^*} \right] \times \left[\pi_i^{\tilde{k}} - \pi_i^{\tilde{k}^*} \right] \geq 0, \quad \forall \pi_i^{\tilde{k}} \geq 0, \quad (23)$$

from which it follows that the equilibrium conditions (13) must hold.

Similarly, let $x_p^k = x_p^{k^*}$, $\forall k, \forall p$; and $\rho_p^k = \rho_p^{k^*}$, $\forall k \neq \tilde{k}$, and $\forall p \neq \tilde{p}$. Substitution of these values into variational inequality (15) yields:

$$\left[x_{\tilde{p}}^{\tilde{k}^*} - \tilde{d}_{\tilde{p}}^{\tilde{k}}(\rho^*, x^*) \right] \times \left[\rho_{\tilde{p}}^{\tilde{k}} - \rho_{\tilde{p}}^{\tilde{k}^*} \right] \geq 0, \quad \forall \rho_{\tilde{p}}^{\tilde{k}} \geq 0, \quad (24)$$

which implies that the equilibrium conditions (14) must hold.

Sufficiency has been established. \square

We now put variational inequality (15) into standard variational inequality form (cf. Nagurney (1999)): determine $X^* \in \mathcal{K}$, such that:

$$\langle F(X^*), X - X^* \rangle \geq 0, \quad \forall X \in \mathcal{K}, \quad (25)$$

where $\langle \cdot, \cdot \rangle$ denotes the inner product in \mathcal{N} -dimensional Euclidean space, F is a given continuous function from \mathcal{K} to $\mathcal{R}^{\mathcal{N}}$, and \mathcal{K} is a given closed, convex set. $\mathcal{N} = K(n_P + m + n_P)$ for the commodity trade network equilibrium model. We define $X \equiv (x, \pi, \rho)$ and \mathcal{K} remains as previously defined. Also, we define $F(X) \equiv (F^1(X), F^2(X), F^3(X))$, where the components of $F^1(X)$ correspond to the Kn_P elements with a typical p element as preceding the first multiplication sign in (15); the components of $F^2(X)$ correspond to the Km elements with a typical such element as immediately preceding the second multiplication sign, and the components of $F^3(X)$ correspond to the Kn_P elements with a typical element as that element preceding the third multiplication sign.

3.3 Illustrative Examples

We now present two simple hypothetical illustrative examples, inspired by the fresh produce trade from Latin America to the United States. The first example focuses on a single commodity, bananas, to demonstrate the fundamental structure of the model, while the second example extends to two commodities, bananas and watermelons, to illustrate the commodity interactions and shared congestion effects on transportation links.

3.3.1 One Commodity Example with Bananas

In this example, there is a single supply market, $i = \{1\}$, located in Latin America, and a single demand market, $j = \{1\}$, in the US. We choose the fresh produce commodity of bananas and, since there is a single commodity, $k = \{1\}$. Also, there is a single transportation path p_1 , which includes the link through the Panama Canal, with the link, a , for simplicity. Hence, we have $f_a^1 = x_{p_1}^1$.

We first define some quality parameters related to the fresh produce commodity bananas. Yan, Sousa-Gallagher, and Oliveira (2008) explore several quality factors related to banana deterioration, including color change and moisture content. They performed experiments to find the most suitable quality deterioration function for these factors. Here, we focus on the color change attribute to assess banana quality decay, using a zero-order deterioration model. The activation energy and pre-exponential constant parameters for our model are derived from their study's data for various quality attributes. As these parameters are challenging to determine independently, we use the values explicitly provided. The universal gas constant is known to be $R = 8.314 Jmol^{-1}K^{-1}$, and the activation energy is taken as $E_A = 32.39 kJmol^{-1}$, and the pre-determined exponential factor is $A = 0.007 hour^{-1}$. We set the temperature parameter as $T_a^1 = 14^\circ C = 287.15^\circ K$, and we calculate the reaction rate: $\kappa_a^1 = 0.007 hour^{-1}$. Moreover, $t_a^0 = 10.00$ hours, $\alpha_a = 1.00$, $u_a = 1.00$, $\gamma_a = 2.00$, $\eta_a^1 = 1.00$, and $q_1^{01} = 100.00$. Given the data, we define:

$$t_a = 10(1 + (f_a^1)^2) = 10(1 + (x_{p_1}^1)^2) = 10 + 10(x_{p_1}^1)^2.$$

Since $f_a^1 = x_{p_1}^1$, we let the quality of the fresh produce commodity on path p_1 be given by the expression:

$$q_{p_1}^1 = 100 - (0.07(1 + (x_{p_1}^1)^2)) = 99.93 - 0.07(x_{p_1}^1)^2.$$

The supply and demand functions are:

$$s_1^1(\pi) = .1\pi_1^1 + 20.907,$$

$$\tilde{d}_{p_1}^1(\rho, q) = 125 - \rho_{p_1}^1 + q_{p_1}^1,$$

$$\tilde{d}_{p_1}^1(\rho, x) = 125 - \rho_{p_1}^1 + 99.93 - 0.07(x_{p_1}^1)^2 = 224.93 - \rho_{p_1}^1 - 0.07(x_{p_1}^1)^2.$$

The unit cost of transportation, where the parameters are assumed to include time and temperature-related costs, is given by:

$$c_a^1(f, t, T) = f_a^1 + 5, \quad \tilde{C}_{p_1}^1(x, T) = x_{p_1}^1 + 5.$$

Because of the simplicity of this example, we can directly find the equilibrium solution according to the variational inequality (15) or through the corresponding network equilibrium conditions (12), (13), and (14). Using the equilibrium conditions, we obtain the following system of equations, assuming a positive path flow and positive supply and demand market prices at the equilibrium:

$$\pi_1^{1*} + \tilde{C}_{p_1}^1(x^*, T) - \rho_{p_1}^* = 0.00,$$

$$s_1^1(\pi^*) - x_{p_1}^{1*} = 0.00,$$

$$x_{p_1}^{1*} - \tilde{d}_{p_1}^1(\rho^*, x^*) = 0.00,$$

which is expanded as:

$$\pi_1^{1*} + x_{p_1}^{1*} - \rho_{p_1}^* = -5.00,$$

$$.1\pi_1^{1*} - x_{p_1}^{1*} = -20.907,$$

$$x_{p_1}^{1*} + \rho_{p_1}^{1*} + 0.07(x_{p_1}^{1*})^2 = 224.93.$$

A solution of this system of equations yields the equilibrium solution: $x_{p_1}^{1*} = 30.37$, $\pi_1^{1*} = 94.63$, and $\rho_{p_1}^{1*} = 130.00$, with $\tilde{C}_{p_1}^1 = 35.37$.

3.3.2 Two Commodity Example with Bananas and Watermelons

We now extend the previous example to include a second commodity, watermelon, to demonstrate the commodity interactions on the shared transportation link. The network structure remains the same. However, we now have two commodities: $k = \{1, 2\}$, where commodity 1 is bananas and commodity 2 is watermelon. Both commodities utilize the same transportation path p_1 , which includes the link through the Panama Canal, denoted by link a . The link flows now account for both commodities: $f_a^1 = x_{p_1}^1$ and $f_a^2 = x_{p_1}^2$.

For the quality parameters, we use the same approach as in the single commodity example. For watermelon, which is also a perishable fresh produce commodity, we use the same activation energy (E_A), pre-exponential constant (A), and universal gas constant (R) as bananas. However, watermelon requires cooler transportation temperatures, typically in the range of $2 - 10^\circ C$ (Marco (2023)). Hence, we set $T_a^2 = 10^\circ C = 283.15^\circ K$. Using equation (4), we calculate the reaction rate for watermelon as $\kappa_a^2 = 0.0069 \text{hour}^{-1}$. Since the calculated value is very close to that of bananas, we use $\kappa_a^2 = 0.007 \text{hour}^{-1}$ for simplicity. The initial quality levels at the supply market are $q_1^{01} = q_1^{02} = 100.00$.

The key feature of the commodity model is that the transportation time on the link now depends on the total flow of both commodities. According to equation (6), the time delay function becomes:

$$t_a = 10 \left(1 + (\eta_a^1 f_a^1 + \eta_a^2 f_a^2)^2 \right) = 10 \left(1 + (x_{p_1}^1 + x_{p_1}^2)^2 \right) = 10 + 10 (x_{p_1}^1 + x_{p_1}^2)^2,$$

where $\eta_a^1 = \eta_a^2 = 1.00$, $\alpha_a = 1.00$, $u_a = 1.00$, and $\gamma_a = 2.00$. Note that the transportation time on the link is now the same for both commodities, as different commodities transported on the same link contribute to congestion and experience the same time delay. Since both commodities have the same decay rate, the quality on path p_1 for bananas and watermelon is the same and is given by:

$$q_{p_1}^k = 100 - 0.07 \left(1 + (x_{p_1}^1 + x_{p_1}^2)^2 \right) = 99.93 - 0.07 (x_{p_1}^1 + x_{p_1}^2)^2, \quad k = 1, 2.$$

The supply and demand functions for bananas remain as defined in the single commodity example. For watermelon, the supply function at the supply market and the demand function on path p_1 are:

$$\begin{aligned} s_1^2(\pi) &= .08\pi_1^2 + 15.50, \\ \tilde{d}_{p_1}^2(\rho, q) &= 110 - \rho_{p_1}^2 + q_{p_1}^2, \\ \tilde{d}_{p_1}^2(\rho, x) &= 110 - \rho_{p_1}^2 + 99.93 - 0.07 (x_{p_1}^1 + x_{p_1}^2)^2 = 209.93 - \rho_{p_1}^2 - 0.07 (x_{p_1}^1 + x_{p_1}^2)^2. \end{aligned}$$

The unit cost of transportation for bananas remains as in the single commodity example. For watermelon, we have:

$$c_a^2(f, t, T) = f_a^2 + 4.5, \quad \tilde{C}_{p_1}^2(x, T) = x_{p_1}^2 + 4.5.$$

Using the equilibrium conditions (12), (13), and (14), we obtain the following system of equations, assuming positive path flows and positive supply and demand market prices at the equilibrium:
For commodity 1:

$$\begin{aligned}\pi_1^{1*} + \tilde{C}_{p_1}^1(x^*, T) - \rho_{p_1}^{1*} &= 0.00, \\ s_1^1(\pi^*) - x_{p_1}^{1*} &= 0.00, \\ x_{p_1}^{1*} - \tilde{d}_{p_1}^1(\rho^*, x^*) &= 0.00.\end{aligned}$$

For commodity 2:

$$\begin{aligned}\pi_1^{2*} + \tilde{C}_{p_1}^2(x^*, T) - \rho_{p_1}^{2*} &= 0.00, \\ s_1^2(\pi^*) - x_{p_1}^{2*} &= 0.00, \\ x_{p_1}^{2*} - \tilde{d}_{p_1}^2(\rho^*, x^*) &= 0.00.\end{aligned}$$

This system can be expanded as:

$$\begin{aligned}\pi_1^{1*} + x_{p_1}^{1*} - \rho_{p_1}^{1*} &= -5.00, \\ .1\pi_1^{1*} - x_{p_1}^{1*} &= -20.907, \\ x_{p_1}^{1*} + \rho_{p_1}^{1*} + 0.07(x_{p_1}^{1*} + x_{p_1}^{2*})^2 &= 224.93, \\ \pi_1^{2*} + x_{p_1}^{2*} - \rho_{p_1}^{2*} &= -4.5, \\ .08\pi_1^{2*} - x_{p_1}^{2*} &= -15.50, \\ x_{p_1}^{2*} + \rho_{p_1}^{2*} + 0.07(x_{p_1}^{1*} + x_{p_1}^{2*})^2 &= 209.93.\end{aligned}$$

A solution of this system of equations yields the equilibrium solution: $x_{p_1}^{1*} = 24.81$, $x_{p_1}^{2*} = 18.48$, $\pi_1^{1*} = 39.08$, $\pi_1^{2*} = 37.25$, $\rho_{p_1}^{1*} = 68.89$, and $\rho_{p_1}^{2*} = 60.23$, with $\tilde{C}_{p_1}^1 = 29.81$ and $\tilde{C}_{p_1}^2 = 22.98$.

This two-commodity example demonstrates several important features of the model. First, the introduction of watermelon as a second commodity using the shared transportation link results in significant congestion effects. The transportation time more than doubles from 9, 233.37 hours in the single commodity case to 18, 750.24 hours in the two-commodity case. This dramatic increase arises because the time delay function depends on the total flow of both commodities, $(x_{p_1}^{1*} + x_{p_1}^{2*})^2$, compared to $(x_{p_1}^{1*})^2$ in the single commodity example. Second, the banana flow decreases from 30.37 to 24.81 when watermelon is introduced, as both commodities contribute to the congestion on the shared link. Third, the equilibrium supply prices for both commodities are substantially lower in the two-commodity case ($\pi_1^{1*} = 39.08$ and $\pi_1^{2*} = 37.25$) compared to the single commodity banana price ($\pi_1^{1*} = 94.63$), reflecting the impact of increased transportation times and reduced final quality on market equilibrium. Fourth, demand prices also decrease significantly from $\rho_{p_1}^{1*} = 130.00$ to $\rho_{p_1}^{1*} = 68.89$ and $\rho_{p_1}^{2*} = 60.23$, as consumers are willing to pay less for products that arrive with lower quality. Finally, the severe congestion leads to quality levels that become negative ($q_{p_1}^1 = q_{p_1}^2 = -31.25$) compared to $q_{p_1}^1 = 35.37$ in the single commodity example, indicating that the transportation link is operating well beyond its efficient upper bound and that the fresh produce would be completely spoiled.

4. Commodity Quality Trade Network Performance Measures

In this section, we provide commodity quality trade network performance measures. Although network performance measures have been proposed for many equilibrium problems from transportation networks to supply chains; for some background see the book by Nagurney and Qiang (2009), assessment of network performance in a trade equilibrium context, notably a spatial price equilibrium one, has been limited to-date. For example, we are only aware of the work by Nagurney et al. (2024b) that introduced an international trade network performance measure and network importance indicators for a commodity international trade network equilibrium model under a spectrum of disruptions in disasters. However, that work did not include quality of commodities, as we do here. Also, since fresh produce quality can sometimes be used a proxy for nutrition as in the case of vitamin C content (cf. Besik and Nagurney (2017)), the measures that we propose here are also relevant to food security.

The performance measures are categorized as being supply-based, demand-based, or network-based, and within each such category we have an individual commodity measure and then a full set of commodities measure. We note that the q_p^{k*} in expressions (26) through (31) below are calculated according to (11) but with each q_p^k evaluated at the equilibrium values x_p^{k*} , $\forall k, \forall p$.

4.1 Individual Commodity Supply-Based Quality Measure

We are interested in quantifying how effective supply markets are from a commodity quality perspective, also with respect to the price(s) that consumers will pay. We consider the performance to be better if the overall quality times the quantity is higher and at a lower price. Of course, the demand market price of a commodity is also of influence, through the equilibrium conditions, and the cost on the transportation routes. The functional form of our performance measures is designed to capture both the quality of delivered commodities and their affordability for consumers. The numerator represents the effective quantity, while accounting for quality, since higher quality shipments provide greater value than equal volumes of lower quality commodities. Dividing the numerator by the demand price incorporates the affordability dimension as a given quality-adjusted volume indicates better quality performance when it is available at lower prices.

In particular, we have the following individual commodity supply-based quality measure, $\mathcal{E}_S^{k,i}$, for commodity k and supply market i :

$$\mathcal{E}_S^{k,i} = \frac{1}{n_{P^i}} \sum_{p \in P^i} \frac{x_p^{k*} q_p^{k*}}{\rho_p^{k*}}, \quad k = 1, \dots, K; i = 1, \dots, m. \quad (26)$$

4.2 Full Set of Commodities Supply-Based Quality Measure

Expanding the individual supply-based quality measure in (26) to all commodities, we obtain the full set of commodities supply-based quality measure, \mathcal{E}_S^i , for supply market i :

$$\mathcal{E}_S^i = \frac{1}{K n_{P^i}} \sum_{k=1}^K \sum_{p \in P^i} \frac{x_p^{k*} q_p^{k*}}{\rho_p^{k*}}, \quad i = 1, \dots, m. \quad (27)$$

Once the values are obtained for either (26) and/or (27) one can then rank the supply markets in terms of their performance in providing quality fresh produce to consumers. Of course, it is important to recognize that the quality that reaches the consumers is dependent on the transportation network.

4.3 Individual Commodity Demand-Based Quality Measure

We now provide the measures from the demand side.

Specifically, the individual commodity demand-based quality measure, $\mathcal{E}_D^{k,j}$, for commodity k and demand market j is given by:

$$\mathcal{E}_D^{k,j} = \frac{1}{n_{P_j}} \sum_{p \in P_j} \frac{x_p^{k*} q_p^{k*}}{\rho_p^{k*}}, \quad k = 1, \dots, K; j = 1, \dots, n. \quad (28)$$

4.4 Full Set of Commodities Demand-Based Quality Measure

Expanding the measure in (28) over all commodities yields the following measure, \mathcal{E}_D^j , for demand market j :

$$\mathcal{E}_D^j = \frac{1}{K n_{P_j}} \sum_{k=1}^K \sum_{p \in P_j} \frac{x_p^{k*} q_p^{k*}}{\rho_p^{k*}}, \quad j = 1, \dots, n. \quad (29)$$

The above demand-based measures are very relevant since they capture the quality/price performance of commodities at the demand markets, which is where the purchasing (and consumption) takes place. One can then rank the demand markets and see which ones perform better for consumers from a quality standpoint.

Finally, we can assess the performance of the full trade network from both individual commodity and full commodity perspectives as in the measures below.

4.5 Individual Commodity Network-Based Quality Measure

For each individual commodity k we define the network-based measure, $\mathcal{E}_{Network}^k$, as:

$$\mathcal{E}_{Network}^k = \frac{1}{n_P} \sum_{p \in P} \frac{x_p^{k*} q_p^{k*}}{\rho_p^{k*}}, \quad k = 1, \dots, K. \quad (30)$$

4.6 Full Set of Commodities Network-Based Quality Measure

The assessment of the full trade network over all the commodities can be captured in the network-based measure, $\mathcal{E}_{Network}$, as:

$$\mathcal{E}_{Network} = \frac{1}{Kn_P} \sum_{k=1}^K \sum_{p \in P} \frac{x_p^{k*} q_p^{k*}}{\rho_p^{k*}}. \quad (31)$$

5. Numerical Examples

In this section, we present a series of numerous examples focusing on the banana trade. All the examples are solved using the modified projection method (Korpelevich (1977)) implemented in MATLAB on a Mac system at the University of Massachusetts Amherst. The algorithm is deemed to have converged if the absolute differences between consecutive iterates of all variables stay are less than or equal to 10^{-7} .

Bananas are a significant part of the global agricultural economy. They are widely consumed and serve as key sources of potassium and vitamin A for about 400 million people in cultivating regions (Banana Link (2024)). Production grew from 97 million tons in 2008 to nearly 120 million tons in 2020 (FAOSTAT (2022)). Although most bananas are consumed locally, about 20% were exported in 2020 (FAOSTAT (2024), Banana Link (2024)). However, total exports declined from 20.4 million tons in 2021 to about 19.1 million tons in 2022 (Food and Agriculture Organization of the United Nations (2023), Besik and Nagurney (2025)).

In 2020, the top banana exporters included Ecuador, the Philippines, and Costa Rica, with exports of about 7, 3.1, and 2.6 million tons, respectively (UN Comtrade Database (2022)). Ecuador, Costa Rica, and Colombia increased their banana exports by about 6%, 21%, and 7%, respectively, between 2019 and 2020 (Food and Agriculture Organization of the United Nations (2021)). The major importers included the European Union, the United States, and China, with 5.2, 4.7, and 1.8 million tons, respectively (UN Comtrade Database (2022)). Banana demand rose by 1.7% from 2019 to 2020, especially in the European Union and the United States (Food and Agriculture Organization of the United Nations (2021), Research and Markets (2019)). Russia was Ecuador’s top banana destination, taking 20% of its exports (Cabezas (2022)).

Our numerical examples examine banana shipments from Ecuador and Costa Rica to the European Union, the United States, and Russia via the Panama Canal. The functions in these examples mainly derive from 2022 data in the FAOSTAT (2024) database. According to this database, Ecuador exported 6.87 million tons in 2022, of which 1.16 million went to the United States (17%), 1.59 million (23%) to the European Union, and 1.59 million (23%) to Russia. Costa Rica, the second largest banana exporter in 2021 (Food and Agricultural Organization of the United Nations (2021)), exported 2.05 million tons in 2022, including 0.63 million tons to the United States and 0.98 million tons to the European Union, but only 1,204 tons to Russia.

The transportation cost from Ecuador to the United States averages 2,945 dollars per container (133 dollars per ton), while the cost to the European Union is approximately 2,962.50 euros per

container (145 dollars per ton) (BR Logistics (2023a)). For Costa Rica, the shipping cost to the United States is 2,980 dollars per container (135 dollars per ton), and to the European Union, 4,250 euros per container (208 dollars per ton) (BR Logistics (2023b)). From Ecuador to Russia, the cost per container is approximately 3,477 dollars (158 dollars per ton), and from Costa Rica to Russia: 3,214 dollars (146 dollars per ton) (FWFreight (2024)). Note that these transportation costs reflect the average cost of each path, representing the complete transportation route between a supply and demand market, which is further broken down into individual links. Each link denotes a specific mode of transportation, contributing to the overall transportation cost. In the above data, “dollars” refers to U.S. dollars.

The Panama Canal is essential to global trade, especially for time-sensitive commodities such as bananas. The Panama Canal is particularly vital for trade involving the Americas, providing a direct connection between the Pacific and Atlantic Oceans. Recently, the Panama Canal’s capacity has been severely constrained by drought, due to lower water levels in Gatun Lake, with daily vessel throughput reduced from about 38 ships to 24 (Ruiz and Shintani (2024)). As the Panama Canal becomes increasingly congested, more vessels are forced to detour around the southern tip of South America (Ruiz and Shintani (2024)). In this analysis, we incorporate these vulnerabilities by considering maritime routes through Panama and examining how the associated drought impacts the banana trade.

5.1 Example 1: Baseline Scenario and Congestion Specification Variants

Example 1 serves as a baseline scenario, with the network topology for Examples 1 and 2 illustrated in Figure 2. In this example, there are two supply markets, $i = \{1, 2\}$, Supply Market 1 in Ecuador and Supply Market 2 in Costa Rica. A single demand market, $j = \{1\}$, Demand Market 1, is located in the European Union. Also, there is a single fresh commodity that of bananas, with $k = \{1\}$. The trade network includes two transportation paths, $\{p_1, p_2\}$, with path p_1 going from Ecuador to the European Union and path p_2 from Costa Rica to the European Union. Each path is comprised of three links. Specifically, path $p_1 = (a, b, c)$, where link a represents rail transportation from Supply Market 1 to the port of Guayaquil in Ecuador, link b represents maritime shipment from this port to the port of Rotterdam in the European Union via the Panama Canal, and link c covers rail transport from the European port to Demand Market 1. For path $p_2 = (d, e, c)$, link d is rail transport from Supply Market 2 to the Port of Quepos, one of the primary Costa Rican ports for exporting bananas (Joshi (2022)) on the Pacific Coast of Costa Rica, with further transportation through the Panama Canal to reach Europe. Subsequently, link e is maritime shipment from this port to the Rotterdam port. The intermediate nodes G , Q , and R , respectively, represent the ports in Ecuador, Costa Rica, and the European Union, as shown in Figure 2. Following the conservation of flow equation (9), the link flows are related to the path flows thus: $f_a^1 = f_b^1 = x_{p_1}^1$, $f_c^1 = x_{p_1}^1 + x_{p_2}^1$, $f_d^1 = f_e^1 = x_{p_2}^1$.

For the quality parameters, as mentioned in the Illustrative Example, we focus on the color change attribute to assess banana quality decay using a zero-order deterioration model. Based on

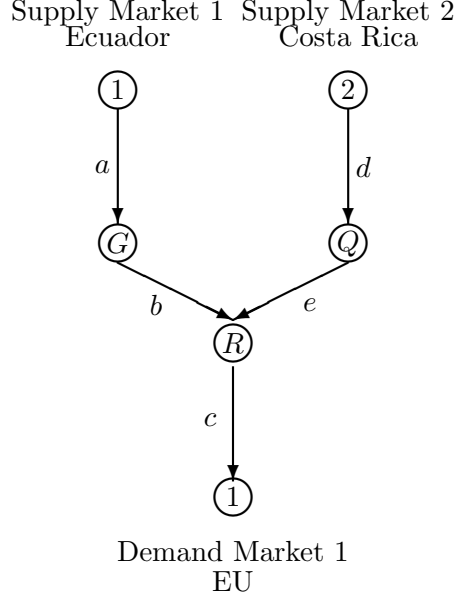


Figure 2: The Banana Trade Network Topology for Examples 1 and 2

the data used in the Illustrative Example and (4), the calculated reaction rate is $\kappa_a^1 = 0.007 \text{hour}^{-1}$ and is fixed for all links in the following examples.

Example 1 corresponds to the baseline scenario prior to any drought-induced impacts on the Panama Canal. Accordingly, the maritime links *b* and *e* each have an upper bound on the volume of shipment of bananas of $u_b = u_e = 3,000,000$. For the rail transportation links, we assume that $u_a = 5,000,000$ and $u_d = u_c = 3,000,000$. For the free-flow transportation time, we have that: $t_a^0 = t_d^0 = t_c^0 = 15.00$ hours, and $t_b^0 = t_e^0 = 140.00$ hours. The initial quality levels of the bananas at the supply markets are assumed to all be 100.00, denoted as $q_1^{01} = q_2^{01} = 100.00$. Furthermore, the additional parameters in (6) are: $\alpha_a = \alpha_b = \alpha_c = \alpha_d = \alpha_e = 2.00$, $\gamma_a = \gamma_b = \gamma_c = \gamma_d = \gamma_e = 4.00$, $\eta_b^1 = \eta_e^1 = 1.00$ and $\eta_a^1 = \eta_c^1 = \eta_d^1 = 2.00$.

Based on these data inputs, the time expressions for the links, in hours, (cf. (6)), take the following form for this example:

$$\begin{aligned}
 t_a^1 &= 15 \left(1 + 2 \left(\frac{2f_a^1}{5 \times 10^6} \right)^4 \right) = 15 \left(1 + 2 \left(\frac{2x_{p_1}^1}{5 \times 10^6} \right)^4 \right), \\
 t_b^1 &= 140 \left(1 + 2 \left(\frac{f_b^1}{3 \times 10^6} \right)^4 \right) = 140 \left(1 + 2 \left(\frac{x_{p_1}^1}{3 \times 10^6} \right)^4 \right), \\
 t_c^1 &= 15 \left(1 + 2 \left(\frac{2f_c^1}{3 \times 10^6} \right)^4 \right) = 15 \left(1 + 2 \left(\frac{2(x_{p_1}^1 + x_{p_2}^1)}{3 \times 10^6} \right)^4 \right), \\
 t_d^1 &= 15 \left(1 + 2 \left(\frac{2f_d^1}{3 \times 10^6} \right)^4 \right) = 15 \left(1 + 2 \left(\frac{2x_{p_2}^1}{3 \times 10^6} \right)^4 \right),
 \end{aligned}$$

$$t_e^1 = 140 \left(1 + 2 \left(\frac{f_e^1}{3 \times 10^6} \right)^4 \right) = 140 \left(1 + 2 \left(\frac{x_{p_2}^1}{3 \times 10^6} \right)^4 \right).$$

The expressions for the final banana quality on the paths according to (7) are: $q_{p_1}^1 = 100 - 0.007(t_a^1 + t_b^1 + t_c^1)$, $q_{p_2}^1 = 100 - 0.007(t_d^1 + t_e^1 + t_c^1)$.

We now present the supply functions for the two supply markets, the demand functions associated with the bananas on each path, along with the link and path unit transportation costs functions.

The supply functions for the Supply Market 1 in Ecuador and the Supply Market 2 in Costa Rica, in tons, are:

$$s_1^1(\pi) = 2844.76\pi_1^1 + 600000, \quad s_2^1(\pi) = 1583.67\pi_2^1 + 300000.$$

The demand functions associated with the two paths, in tons, are:

$$\tilde{d}_{p_1}^1(\rho, q) = 600000 - 1080.13\rho_{p_1}^1 + 17351.93q_{p_1}^1, \quad \tilde{d}_{p_2}^1(\rho, q) = 300000 - 582.12\rho_{p_2}^1 + 11012.94q_{p_2}^1.$$

From equations (7) and (9), one can see that the final demand functions are inherently dependent on the path flows, as noted after (11).

The unit transportation costs associated with the links and paths, where the parameters are assumed to include temperature-related costs of temperature-controlled containers, in dollars per ton, are given by:

$$\begin{aligned} c_a^1(f, t, T) &= 0.00002f_a^1 + 0.2t_a^1 + 10, & c_b^1(f, t, T) &= 0.00005f_b^1 + 0.2t_b^1 + 25, \\ c_c^1(f, t, T) &= 0.00002f_c^1 + 0.2t_c^1 + 10, & c_d^1(f, t, T) &= 0.00002f_d^1 + 0.2t_d^1 + 10, \\ c_e^1(f, t, T) &= 0.00005f_e^1 + 0.2t_e^1 + 20, \\ \tilde{C}_{p_1}^1(x, T) &= c_a^1 + c_b^1 + c_c^1, & \tilde{C}_{p_2}^1(x, T) &= c_d^1 + c_e^1 + c_c^1. \end{aligned}$$

In the cost function for the maritime link from Ecuador to the European Union (link b), a larger fixed cost term is adopted compared to that from Costa Rica (link e), which accounts for Ecuador's relatively greater distance to the Panama Canal, reflecting the higher transportation cost. The computed equilibrium commodity path flows, banana quality, supply prices, and demand prices (in dollars) are reported in Table 2. Table 3 reports the commodity supplies, demands, and unit path transportation costs at the equilibrium for Example 1, denoted in tons, tons, and dollars per ton, respectively.

In the baseline nonlinear congestion scenario ($\gamma = 4$), Ecuador and Costa Rica supply bananas to the European Union along their respective transportation paths without upper bound reductions or extended transportation times. The equilibrium path flows in Table 2, which align closely with

Table 2: Computed Equilibrium Values of Path Flows, Banana Quality, Supply Prices, and Demand Prices for Example 1 Under Alternative Congestion Specifications

Computed Equilibrium Values	Example 1 ($\gamma = 4$)	Example 1 ($\gamma = 1$)	Example 1 ($\alpha = 0$)
$x_{p_1}^{1*}$	1,585,010.10	1,598,848.82	1,648,841.54
$x_{p_2}^{1*}$	976,043.38	989,495.51	1,011,423.39
$q_{p_1}^{1*}$	96.83	97.26	98.81
$q_{p_2}^{1*}$	96.96	97.66	98.81
π_1^{1*}	346.25	351.12	368.69
π_2^{1*}	426.88	435.38	449.22
$\rho_{p_1}^{1*}$	643.74	637.84	616.31
$\rho_{p_2}^{1*}$	673.11	663.19	647.22

the real-world data on 2022 bananas exports of 1.59 and 0.98 million tons to the European Union, respectively (FAOSTAT (2024)), are substantial. Using equation (6), the time for transportation of the bananas from Ecuador and Costa Rica to the European Union are calculated as 451.60 hours (approximately 19 days) and 433.45 hours (about 18 days), respectively. These values correspond closely to those reported by Fluentcargo (2024) and Maersk (2024), which indicate a typical shipping duration of three weeks from Ecuador and Costa Rica to the European Union. These results reflect conditions where adequate upper bounds on links, reasonable transportation durations, and high initial quality levels of the bananas all support robust trade volumes. Notably, the high final quality levels in Example 1 (both exceeding 96) confirm that, under normal transportation upper bounds and times, the deterioration of the quality of the bananas is minimal. This result supports that efficient transportation routes help to maintain freshness; thereby, resulting in the delivery of high-quality fresh produce commodities, which, in this case, are bananas to the demand market.

The supply prices in Table 2 reveal that Ecuador has a lower equilibrium supply price as compared to Costa Rica, with both being in a range similar to actual prices reported by the FAOSTAT (2024) database. According to this data, and documented in Besik and Nagurney (2025), in 2021, the supply prices for bananas were reported at 321.1 and 464.3 dollars per ton in Ecuador and Costa Rica, respectively. In 2022, the supply prices in Ecuador declined to 276.4 dollars per ton. Demand prices associated with both transportation paths from Ecuador and Costa Rica to the European Union also settle near the real import prices with reference the Food and Agriculture Organization of the United Nations (2023), reporting the average import price of bananas in the European Union at 696 dollars per ton. These results reinforce the practical relevance of the Example 1 solution.

In addition to the baseline example with nonlinear congestion functions with $\gamma = 4$, we also consider two alternative representations of the time delay functions for comparison purposes. The first one assumes linear congestion with $\gamma = 1$, in which transportation times increase proportionally with shipment volumes. The second assumes no-congestion effects with $\alpha = 0$, so that transportation times remain fixed at their free-flow levels and do not depend on flows or link upper

bounds.

Compared to the nonlinear congestion function case, the linear and no-congestion cases yield systematically higher shipment volumes and higher final quality levels, driven by shorter transportation times. Under the linear congestion function ($\gamma = 1$), the transportation times decline to 390.17 hours for path p_1 and 333.90 hours for path p_2 , leading to modest increases in equilibrium flows and improvements in banana quality relative to the nonlinear function. These effects are further amplified under the no-congestion model ($\alpha = 0$), where transportation times fall sharply to 170.00 hours on both paths, resulting in the highest shipment volumes and final quality. Correspondingly, supply prices increase while demand prices decline, reflecting lower transportation delays and reduced costs of delivering high-quality bananas to the European Union. While the linear and no-congestion cases provide useful benchmarks, they do not account for upper bound limits or congestion effects that are common on heavily used trade routes. In contrast, our model with nonlinear congestion link cost functions provides a more realistic representation, since transportation times, prices, and quality deterioration adjust accordingly in response to shipment volumes.

Table 3: Function Values at the Equilibrium for Example 1 Under Alternative Congestion Specifications

Functions	Example 1 ($\gamma = 4$)	Example 1 ($\gamma = 1$)	Example 1 ($\alpha = 0$)
s_1^1	1,585,010.10	1,598,848.82	1,648,841.54
s_2^1	976,043.38	989,495.51	1,011,423.39
$d_{p_1}^1$	1,585,010.10	1,598,848.82	1,648,841.54
$d_{p_2}^1$	976,043.38	989,495.51	1,011,423.39
$C_{p_1}^1$	297.49	286.72	247.62
$C_{p_2}^1$	246.23	227.81	198.00

Table 3 indicates that the transportation cost from Ecuador to the European Union in the nonlinear congestion case is higher than that from Costa Rica, which can be explained by higher banana shipments and the longer transportation time between Ecuador and the European Union. The equilibrium conditions (12) - (14) hold accurately.

Table 4: Banana Quality Trade Performance Measures for Example 1 Under Alternative Congestion Specifications

Performance Measures	Example 1 ($\gamma = 4$)	Example 1 ($\gamma = 1$)	Example 1 ($\alpha = 0$)
$\mathcal{E}_S^{1,1}$	238,433.08	243,819.25	264,347.71
$\mathcal{E}_S^{1,2}$	140,603.62	145,714.61	154,410.07
$\mathcal{E}_D^{1,1}$	189,518.35	194,766.93	209,378.89
$\mathcal{E}_{Network}^1$	189,518.35	194,766.93	209,378.89

Table 4 reports the commodity supply-based, demand-based, and the network-based quality

measures for Example 1 under different congestion specifications. From the perspective of the quality-based performance measures, we note that, in the nonlinear model, the supply and demand quality measures are notably high, signifying that the banana trade network is performing effectively in moving high quality bananas at prices consumers are willing to pay. However, Ecuador has a higher supply-based quality measure, which can be attributed to the higher volume of bananas shipped to the European Union and lower demand prices on its transportation path.

A comparison across the congestion function cases in Tables 3 and 4 further highlights how the mathematical representation of transportation delays shapes cost and quality performance measures. Under the linear and no-congestion cases, unit path transportation costs decline relative to the nonlinear congestion model, reflecting shorter transportation times and the lack of sensitivity to the volume-to-upper bound ratio on the links. At the same time, the supply-based, demand-based, and network-based quality performance measures increase, suggesting that ignoring or simplifying congestion effects leads to an overestimation of quality performance. Although the linear and no-congestion cases demonstrate lower incurred costs and higher quality performance measures, they do so by assuming that transportation times are either invariant to flow or change linearly with volume, thus understating the increasing delays that characterize congested transportation routes.

5.2 Example 2: Example 1 but with Upper Bound Reductions on Maritime Transportation Links via the Panama Canal and Increases in Free-Flow Transportation Times and Congestion Specification Variants

In Example 2, we analyze the effect of drought conditions in the Panama Canal, as occurred in 2023-2024. As noted earlier, the number of daily ship transits through the Panama Canal had been reduced from 38 to 24, representing almost a 36% decline in normal capacity (O'Dell (2024), Ruiz and Shintani (2024)). We mirror this by reducing the upper bounds of maritime links by 40%, so that: $u_b = u_e = 1,800,000$. Following the approach presented in Besik and Nagurney (2025), we set new free-flow times for links b and e , as $t_b^0 = t_e^0 = 500.00$ hours. The remaining data are as in Example 1. The equilibrium solutions for Example 2 and the function values at the equilibrium are displayed in Tables 5 and 6, respectively.

Table 5: Computed Equilibrium Values of Path Flows, Banana Quality, Supply Prices, and Demand Prices for Example 2 Under Alternative Congestion Specifications

Computed Equilibrium Values	Example 2 ($\gamma = 4$)	Example 2 ($\gamma = 1$)	Example 2 ($\alpha = 0$)
$x_{p_1}^{1*}$	1,433,093.85	1,379,142.85	1,567,285.18
$x_{p_2}^{1*}$	928,741.62	888,686.13	963,030.91
$q_{p_1}^{1*}$	92.16	90.49	96.29
$q_{p_2}^{1*}$	94.47	92.39	96.29
π_1^{1*}	292.85	273.89	340.02
π_2^{1*}	397.02	371.72	418.66
$\rho_{p_1}^{1*}$	709.29	732.40	651.34
$\rho_{p_2}^{1*}$	707.20	736.65	682.68

In Example 2, with reduced upper bounds on the routes passing via the Panama Canal and increased free-flow transportation time, the equilibrium solution is significantly different from the one in Example 1. As reported in Table 5, under the nonlinear congestion function ($\gamma = 4$), the equilibrium shipment volumes drop dramatically from their values in Example 1 for both Ecuador and Costa Rica by 9.58% and 4.84%, respectively. This result parallels recent real-world trends, where Ecuadorian banana exports have declined in the first two months of 2024 due to the Panama Canal congestion as one factor, leading to decreases in both the quality and the quantity of bananas (Tridge (2024)). However, Costa Rica, with access to both oceans is less impacted by drought than Ecuador (ProducePay (2023)). Prolonged transportation times directly impact the quality of the bananas, since the transportation times from Ecuador and Costa Rica to the European Union are now 1,119.43 (approximately 46 days) and 789.68 (approximately 32 days), respectively. These extended durations match real-world reports of severe Panama Canal delays due to drought. For instance, Tomorrow’s Affairs (2023) notes that exporters in South America have faced waits of several weeks. Similarly, O’Dell (2024) indicates wait times ranging from 2 to 55 days, depending on vessel type and direction, and U.S. Energy Information Administration (2023) documents 17-day minimum waits for Neopanamax ships. These observations support the prolonged transportation times seen in the results for Example 2, confirming the realistic nature of the computed results. The final banana quality values decrease appreciably with now: $q_{p_1}^{1*} = 92.16$ and $q_{p_2}^{1*} = 94.47$, with lower quality for bananas originating from Ecuador, because the longer transportation time leads to greater quality deterioration.

Table 6: Function Values at the Equilibrium for Example 2 Under Alternative Congestion Specifications

Functions	Example 2 ($\gamma = 4$)	Example 2 ($\gamma = 1$)	Example 2 ($\alpha = 0$)
s_1^1	1,433,093.80	1,379,142.85	1,567,285.18
s_2^1	928,741.62	888,686.13	963,030.91
$\tilde{d}_{p_1}^1$	1,433,093.80	1,379,142.85	1,567,285.18
$\tilde{d}_{p_2}^1$	928,741.62	888,686.13	963,030.91
$\tilde{C}_{p_1}^1$	416.44	458.51	311.32
$\tilde{C}_{p_2}^1$	310.18	364.93	264.02

Observe that the banana supply prices in both Ecuador and Costa Rica decline (15.42% and 6.99%) from their values in Example 1, which is associated with lower shipments to the European Union. As a direct consequence of the decline in shipment volumes, the demand prices on both paths for the banana flows increase, by 10.18% and 5.06% as compared to their values in Example 1. Notably, the lower supply prices, coupled with the higher demand prices, reflect the economic costs for both producers and consumers with farmers producing fewer bananas, and at lower prices, and with consumers paying more for lower quality bananas than in Example 1.

To further assess the role of congestion modeling under reduced upper bounds and increased free-flow time, we compare the nonlinear congestion formulation with linear and no-congestion models

using the same data. As expected, the no-congestion case ($\alpha = 0$) yields the shortest transportation times (530.00 hours on both paths), highest final quality, and largest shipment volumes, since it treats the increased free-flow time as fixed and ignores flow-dependent delays.

The comparison between linear and nonlinear congestion function results, however, reveals an important distinction. Under the linear specification ($\gamma = 1$), congestion penalties accumulate in direct proportion to the flow-to-upper bound ratio even at low flow levels. In Example 2, with reduced upper bounds ($u_b = u_e = 1,800,000$) and increased free-flow times ($t_b^0 = t_e^0 = 500.00$) equilibrium flows, under $\gamma = 1$, represent 76-78% of link upper bounds. At these flow levels, the linear congestion term, for link b as $\alpha_b \left(\frac{\eta_b^1 f_b^1}{u_b} \right)$ and for link e as $\alpha_e \left(\frac{\eta_e^1 f_e^1}{u_e} \right)$, directly translates to substantial time penalties. This results in the longest transportation times (1,358.09 hours on path p_1 and 1,086.84 hours on path p_2), exceeding even the nonlinear case. These longer time delays lead to greater quality deterioration, lower equilibrium shipment volumes, lower supply prices, and higher demand prices. In contrast, the nonlinear formulation applies a fourth power function to the flow-to-upper bound ratio. For flows below the upper bound, this exponent substantially reduces the congestion effect. This allows the nonlinear model to accommodate moderately high flows with lower time penalties than the linear specification.

The distinction becomes critical under upper bound reductions and higher free-flow transportation times, where flows must operate at higher utilization rates to meet demand, causing the linear formulation to impose excessive time penalties that reduce equilibrium volumes relative to the nonlinear function. This comparison illustrates that linear congestion functions can overstate delays at moderate-to-high flow levels, whereas nonlinear functions more realistically capture how transportation times remain modest until flows approach link upper bounds, and then increase sharply.

Table 7: Banana Quality Trade Performance Measures for Example 2 Under Alternative Congestion Specifications

Performance Measures	Example 2 ($\gamma = 4$)	Example 2 ($\gamma = 1$)	Example 2 ($\alpha = 0$)
$\mathcal{E}_S^{1,1}$	186,213.03	170,402.28	231,697.46
$\mathcal{E}_S^{1,2}$	124,067.11	111,459.80	135,831.51
$\mathcal{E}_D^{1,1}$	155,140.07	140,931.04	183,764.49
$\mathcal{E}_{Network}^1$	155,140.07	140,931.04	183,764.49

As is clear from the reported solution data for Example 2 in Tables 5 and 6, the equilibrium conditions (12), (13), and (14) are satisfied. Table 6 further shows that unit transportation costs are highest under the linear congestion model and lowest when congestion is not considered. Under linear congestion, transportation costs increase strongly even when shipment volumes are only moderately high, because delays rise proportionally with flows. In contrast, the nonlinear congestion formulation keeps costs relatively lower when flows are below upper bound and only produces large cost increases once the links become heavily utilized. As a result, the nonlinear

model avoids overstating transportation costs under moderate congestion while still capturing sharp cost increases near upper bound limits.

The effect on network performance is stark since the supply-based, demand-based, and network-based quality measures (cf. Table 7) decline substantially as compared to the results for Example 1, reflecting the diminished performance of the banana trade network. It is interesting to see that, although Costa Rica attains a higher final quality and lower demand price on its path to the European Union, its smaller shipment volumes reduce its supply-based quality measure. Conversely, Ecuador ships a larger volume of bananas with a slightly lower quality and a higher demand price, yielding a higher supply-based quality measure in the end. This outcome illustrates how trade-offs among transportation volumes, commodity quality, and demand price collectively determine each supply market quality performance. Example 2 clearly demonstrates the vulnerability of the banana fresh produce trade network to infrastructural and environmental disruptions, with a negative impact on both producers and consumers.

5.3 Example 3: Example 1 with an Additional Demand Market - the United States

Example 3 has the same data as that in Example 1 but with additional data added, as discussed below for the additional Demand Market 2, which is the United States. Please refer to Figure 3. We now have $i = \{1, 2\}$, $j = \{1, 2\}$, and four paths $\{p_1, p_2, p_3, p_4\}$, with the first two paths being as in the preceding two examples and with new paths: $p_3 = (a, f, g)$ and $p_4 = (d, h, g)$. Link f represents maritime shipment from the port in Ecuador to a port in the United States via the Panama Canal (node U in Figure 3); link g corresponds to rail transport from the US port to the demand market in the United States, and link h corresponds to maritime transport from the port of Quepos in Costa Rica to the US port via the Panama Canal. The free-flow transportation times for the added links are: $t_g^0 = 15.00$ hours and $t_f^0 = t_h^0 = 80.00$ hours, due to shorter distances than to the European Union. The transportation upper bounds on the maritime links from Ecuador and Costa Rica to the United States are set to: $u_f = u_h = 2,000,000$, and for the rail transport within the United States to: $u_g = 3,000,000$.

With the new links associated with Demand Market 2, additional parameters in (6) are: $\alpha_f = \alpha_h = \alpha_g = 2.00$, $\gamma_f = \gamma_h = \gamma_g = 4.00$, $\eta_f^1 = \eta_h^1 = 1.00$, and $\eta_g^1 = 2.00$. Since there are additional paths in Example 3, representing banana shipments to the United States, we now have updated link flows as: $f_a^1 = x_{p_1}^1 + x_{p_3}^1$, $f_f^1 = x_{p_3}^1$, $f_g^1 = x_{p_3}^1 + x_{p_4}^1$, $f_d^1 = x_{p_2}^1 + x_{p_4}^1$, $f_h^1 = x_{p_4}^1$.

The new and updated link transportation times according to (6) are:

$$t_a^1 = 15 \left(1 + 2 \left(\frac{2f_a^1}{5 \times 10^6} \right)^4 \right) = 15 \left(1 + 2 \left(\frac{2(x_{p_1}^1 + x_{p_3}^1)}{5 \times 10^6} \right)^4 \right),$$

$$t_f^1 = 80 \left(1 + 2 \left(\frac{f_f^1}{2 \times 10^6} \right)^4 \right) = 80 \left(1 + 2 \left(\frac{x_{p_3}^1}{2 \times 10^6} \right)^4 \right),$$

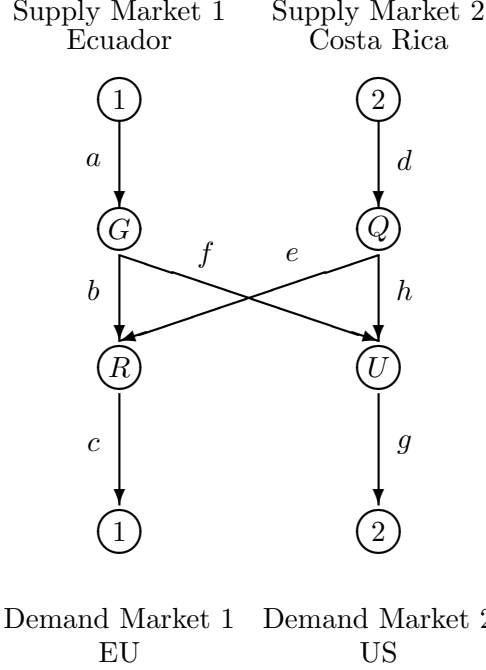


Figure 3: The Banana Trade Network Topology for Example 3 and 4

$$t_g^1 = 15 \left(1 + 2 \left(\frac{2f_g^1}{3 \times 10^6} \right)^4 \right) = 15 \left(1 + 2 \left(\frac{2(x_{p_3}^1 + x_{p_4}^1)}{3 \times 10^6} \right)^4 \right),$$

$$t_d^1 = 15 \left(1 + 2 \left(\frac{2f_d^1}{3 \times 10^6} \right)^4 \right) = 15 \left(1 + 2 \left(\frac{2(x_{p_2}^1 + x_{p_4}^1)}{3 \times 10^6} \right)^4 \right),$$

$$t_h^1 = 80 \left(1 + 2 \left(\frac{f_h^1}{2 \times 10^6} \right)^4 \right) = 80 \left(1 + 2 \left(\frac{x_{p_4}^1}{2 \times 10^6} \right)^4 \right).$$

The final quality expressions for the bananas on the paths from both supply markets to the Demand Market 2 are: $q_{p_3}^1 = 100 - 0.007(t_a^1 + t_f^1 + t_g^1)$, $q_{p_4}^1 = 100 - 0.007(t_d^1 + t_h^1 + t_g^1)$.

The introduction of a new demand market changes the trade network's structure, requiring updates to the supply and demand functions. On the supply side, new markets influence how farmers at the supply markets change their decisions on exports and supply prices. On the demand side, an additional market affects the consumers' willingness to pay and quality preferences as bananas are distributed across a larger network. Updating these functions ensures that such changes are reflected and align with real-world trade dynamics, where market changes impact supply and demand behavior. We, hence, update the existing supply and demand functions according to:

$$s_1^1(\pi) = 5,771.53\pi_1^1 + 1,000,000, \quad s_2^1(\pi) = 2,764.95\pi_2^1 + 500,000,$$

$$\tilde{d}_{p_1}^1(\rho, q) = 600,000 - 1,326.46\rho_{p_1}^1 + 18911.39q_{p_1}^1, \quad \tilde{d}_{p_2}^1(\rho, q) = 300,000 - 594.33\rho_{p_2}^1 + 11,099.71q_{p_2}^1,$$

$$\tilde{d}_{p_3}^1(\rho, q) = 300,000 - 965.81\rho_{p_3}^1 + 14,124.35q_{p_3}^1, \quad \tilde{d}_{p_4}^1(\rho, q) = 100,000 - 667.80\rho_{p_4}^1 + 9,346.74q_{p_4}^1.$$

The unit transportation cost functions associated with new links and paths, in dollars per ton, are given by:

$$c_f^1(f, t, T) = 0.00005f_f^1 + 0.2t_f^1 + 25, \quad c_h^1(f, t, T) = 0.00005f_h^1 + 0.2t_h^1 + 20,$$

$$c_g^1(f, t, T) = 0.00002f_g^1 + 0.2t_g^1 + 10,$$

$$\tilde{C}_{p_3}^1(x, T) = c_a^1 + c_f^1 + c_g^1, \quad \tilde{C}_{p_4}^1(x, T) = c_d^1 + c_h^1 + c_g^1.$$

The computed equilibrium solution and the function values at the equilibrium for Example 3 are displayed in Tables 8 and 9, respectively.

Table 8: Computed Equilibrium Values of Path Flows, Banana Quality, Supply Prices, and Demand Prices for Examples 3 and 4

Computed Equilibrium Values	Example 3	Example 4
$x_{p_1}^{1*}$	1,587,104.01	1,429,341.82
$x_{p_2}^{1*}$	977,105.54	934,565.27
$x_{p_3}^{1*}$	1,163,699.97	994,651.72
$x_{p_4}^{1*}$	631,361.68	574,693.82
$q_{p_1}^{1*}$	96.55	92.02
$q_{p_2}^{1*}$	96.71	94.27
$q_{p_3}^{1*}$	98.36	92.54
$q_{p_4}^{1*}$	98.51	95.45
π_1^{1*}	303.35	246.73
π_2^{1*}	400.90	365.02
$\rho_{p_1}^{1*}$	632.42	686.78
$\rho_{p_2}^{1*}$	667.01	692.90
$\rho_{p_3}^{1*}$	544.22	634.22
$\rho_{p_4}^{1*}$	583.09	625.18

From Table 8, we observe that banana shipments from Ecuador to the United States are higher than exports from Costa Rica to the United States, which complies with the actual shipment volumes of 1.16 and 0.63 million tons noted at the beginning of Section 5 (FAOSTAT (2024)). Moreover, the volumes of shipments from Ecuador and Costa Rica to the European Union are similar to their associated values in Example 1. Turning to prices, Table 8 shows that the Ecuador and Costa Rica equilibrium supply prices are lower than their values in Example 1. Both equilibrium supply prices lie in a range reasonably close to the reported prices in the FAOSTAT(2024) dataset. Meanwhile, the equilibrium demand prices for banana shipments from Ecuador and Costa Rica to the United States closely reflect the actual import prices of bananas in the United States of 532.80 dollars per ton in 2023, consistent with Karst (2024). The demand prices associated with the paths from the supply markets to the European Union in Example 3 are slightly lower than those values in Example 1, which can be due to higher volumes of bananas on paths p_1 and p_2 reaching the European Union as compared to the results in Example 1.

The final quality of the bananas on all paths remains very high in Example 3, reflecting relatively uncongested maritime links and reasonable transportation times. With the further distance from Ecuador and Costa Rica to the European Union than to the United States and higher transportation times given by: 492.10, 469.01, 233.84, and 212.78 hours (approximately 20, 19, 10, and 9 days), respectively, the final quality of the bananas on paths reaching the European Union is slightly lower than that of bananas heading to the United States. These transportation times also align with real-world data - Fluentcargo (2024) indicates that exports from Ecuador to the United States generally take 10 to 15 days, while transit from Costa Rica can be under 10 days. In addition, Portfolio (2015) reports that shipment of bananas from Ecuador to the United States typically takes less than three weeks.

Table 9: Function Values at the Equilibrium for Examples 3 and 4

Functions	Example 3	Example 4
s_1^1	2,750,803.98	2,423,993.54
s_2^1	1,608,467.22	1,509,259.09
$\tilde{d}_{p_1}^1$	1,587,104.01	1,429,341.82
$\tilde{d}_{p_2}^1$	977,105.54	934,565.27
$\tilde{d}_{p_3}^1$	1,163,699.97	994,651.72
$\tilde{d}_{p_4}^1$	631,361.68	574,693.82
$\tilde{C}_{p_1}^1$	329.07	440.06
$\tilde{C}_{p_2}^1$	266.11	327.88
$\tilde{C}_{p_3}^1$	240.87	387.49
$\tilde{C}_{p_4}^1$	182.19	260.16

Table 9 displays the equilibrium function values. The transportation costs from Ecuador and Costa Rica to the United States are lower than the transportation costs from both supply markets to the European Union, which are explained by the transportation distances. These values also closely reflect the actual transportation costs provided earlier in Section 5. From the results in Tables 8 and 9 it is clear that the equilibrium conditions hold.

Table 10: Banana Quality Trade Performance Measures for Examples 3 and 4

Performance Measures	Example 3	Example 4
$\mathcal{E}_S^{1,1}$	226,318.71	168,334.36
$\mathcal{E}_S^{1,2}$	124,172.94	107,447.60
$\mathcal{E}_D^{1,1}$	191,995.15	159,336.93
$\mathcal{E}_D^{1,2}$	158,496.50	116,445.03
$\mathcal{E}_{Network}^1$	175,245.83	137,890.98

Table 10 reveals that Ecuador outperforms Costa Rica on the supply-based quality measure, reflecting Ecuador's larger banana shipments to both demand markets and lower demand prices on those routes. On the demand side, the European Union exhibits a higher quality measure than the United States even with higher demand prices and slightly lower final quality primarily because

greater volumes flow from both supply markets to the European Union. Although these increases in volume boost overall network activity, the network-based quality measure in Example 3 is lower than in Example 1. This decline is likely due to the added paths and complexity within the network, which amplifies transportation times and can erode the final quality of bananas.

5.4 Example 4: Example 3 but with Upper Bound Reductions on Maritime Transportation Links via the Panama Canal and Increases in Free-Flow Transportation Times

In Example 4 (similar to Example 2) we investigate the impact of reductions in transportation link upper bounds, accompanied by an increase in the free-flow transportation times for maritime routes between Costa Rica and Ecuador to the United States and to the European Union. This example has the same data as that in Example 3 except for such changes. Specifically, we reduce the transportation upper bounds of the maritime links by 40%, yielding new upper bounds of: $u_b = u_e = 1,800,000$ and $u_h = u_f = 1,200,000$, while also increasing the free-flow times on these links to account for additional delays, thus: $t_b^0 = t_e^0 = t_h^0 = t_f^0 = 500.00$ hours. We aim to examine the effects on transportation times on the quality degradation of bananas over extended journeys, on cost increments due to increased congestion, and on the resulting shifts in shipment quantities across paths. The remaining data are as in Example 3.

Table 8 presents the equilibrium solution for Example 4, with the corresponding equilibrium function values and quality measures reported in Tables 9 and 10, respectively.

As reported in Table 8, banana flows from Ecuador and Costa Rica to the European Union and the United States drop relative to those in Example 3 by 9.94%, 4.35%, 14.52% and 8.97%, respectively. Transportation times from Ecuador and Costa Rica to the European Union and the United States are now: 1139.16, 818.46, 1,064.47, and 649.29 hours (approximately 47, 34, 44, 27 days), respectively. Moreover, the final banana quality on all paths decreases in Example 4, which is a predictable outcome of longer transportation times and limited upper bounds. However, the final quality stays above 90% even under extensive transportation times. Modern cold-chain technologies as in reefer vessels and/or refrigerated shipping containers can significantly slow ripening and preserve quality, even during lengthy maritime transit (Port Economics, Management and Policy (2022)). As a result, the computed final quality reflects conditions in which acceptable-quality bananas still reach the demand markets. Supply prices in Ecuador and Costa Rica fall by 18.66% and 8.95%, respectively, whereas demand prices along the paths rise by 8.59%, 3.88%, 16.53%, and 7.21%. Overall, consumers end up paying more for bananas of lower quality.

Equilibrium conditions (12) - (14) are satisfied for this example. Transportation costs on all paths increase relative to those in Example 3, driven by both upper bounds reductions and longer transportation times. According to FreshPlaza (2025), three of Ecuador's major banana shipping companies have imposed an additional charge per container transiting the Panama Canal after the drought. Similarly, as reported by FreshFruitPortal.com (2024), drought and subsequent upper bounds reductions have increased transportation costs, particularly in the first two months of 2024.

In Example 4, Table 10 reveals a significant drop across the supply-based, demand-based, and network-based quality measures as compared to Example 3, underscoring the adverse effects of congested routes. Although Ecuador continues to export more bananas than Costa Rica and thus retains an overall advantage in its supply-based quality measure, congestion and reduced upper bounds negatively impact product freshness, causing a notable decrease in final quality levels. The European Union remains the most robust demand market for quality, as it receives a larger share of banana shipments from both supply markets. Nevertheless, the effect of these disruptions is apparent in the lower network-based measure, demonstrating how disruptions and transportation delays reduce overall banana trade performance.

5.5 Example 5: Addition of Demand Market 3 - Russia - to Example 3 with Updated and added Functions

Example 5 is derived from Example 3 by adding Demand Market 3 - Russia, as depicted in Figure 4. The existing supply and demand functions have been updated, and new functions and parameters have been added for new paths from Ecuador and Costa Rica to Russia. Two new paths are defined for bananas exported from Ecuador and Costa Rica to Russia, each consisting of three links: $p_5 = (a, i, j)$ and $p_6 = (d, k, j)$. The index sets are now: $i = \{1, 2\}$, $j = \{1, 2, 3\}$, with paths: $\{p_1, p_2, p_3, p_4, p_5, p_6\}$. Link i corresponds to maritime transportation from the Port of Guayaquil in Ecuador to a port in Russia via the Panama Canal (e.g., Port of Novorossiysk) and entails also traversal of the Atlantic Ocean, transit through the Mediterranean Sea, and the Black Sea. Link j denotes rail transport from the Russian port to the demand market inside Russia, while link k corresponds to maritime transportation from the Port of Quepos in Costa Rica to the Port of Novorossiysk in Russia via the Panama Canal, as per above.

The free-flow transportation times for the added links are: $t_j^0 = 15.00$ hours, and $t_i^0 = t_k^0 = 200.00$ hours, due to the longer route to Russia as compared to paths to the United States and the European Union. The transportation upper bounds on maritime shipments from Ecuador and Costa Rica to Russia are set to: $u_i = 3,000,000$ and $u_k = 20,000$, and for the rail transportation inside Russia to $u_j = 2,000,000$.

Parameters in (6) for the new links are: $\alpha_i = \alpha_k = \alpha_j = 2.00$, $\gamma_i = \gamma_k = \gamma_j = 4.00$, $\eta_i^1 = \eta_k^1 = 1.00$, and $\eta_j^1 = 2.00$.

The link flow expressions considering the addition of Demand Market 3 and the time equations are: $f_a^1 = x_{p_1}^1 + x_{p_3}^1 + x_{p_5}^1$, $f_d^1 = x_{p_2}^1 + x_{p_4}^1 + x_{p_6}^1$, $f_k^1 = x_{p_6}^1$, $f_j^1 = x_{p_5}^1 + x_{p_6}^1$, $f_i^1 = x_{p_5}^1$.

$$t_a^1 = 15 \left(1 + 2 \left(\frac{2f_a^1}{5 \times 10^6} \right)^4 \right) = 15 \left(1 + 2 \left(\frac{2(x_{p_1}^1 + x_{p_3}^1 + x_{p_5}^1)}{5 \times 10^6} \right)^4 \right),$$

$$t_d^1 = 15 \left(1 + 2 \left(\frac{2f_d^1}{3 \times 10^6} \right)^4 \right) = 15 \left(1 + 2 \left(\frac{2(x_{p_2}^1 + x_{p_4}^1 + x_{p_6}^1)}{3 \times 10^6} \right)^4 \right),$$

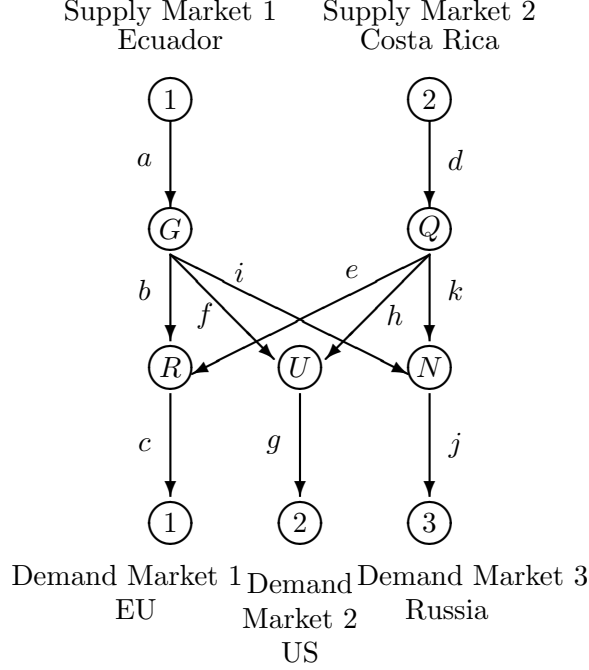


Figure 4: The Banana Trade Network Topology for Example 5 and 6

$$t_k^1 = 200 \left(1 + 2 \left(\frac{f_k^1}{2 \times 10^4} \right)^4 \right) = 200 \left(1 + 2 \left(\frac{x_{p_6}^1}{2 \times 10^4} \right)^4 \right),$$

$$t_j^1 = 15 \left(1 + 2 \left(\frac{2f_j^1}{2 \times 10^6} \right)^4 \right) = 15 \left(1 + 2 \left(\frac{2(x_{p_5}^1 + x_{p_6}^1)}{2 \times 10^6} \right)^4 \right),$$

$$t_i^1 = 200 \left(1 + 2 \left(\frac{f_i^1}{3 \times 10^6} \right)^4 \right) = 200 \left(1 + 2 \left(\frac{x_{p_5}^1}{3 \times 10^6} \right)^4 \right).$$

The final quality levels of the bananas on paths from Supply Markets 1 and 2 to the Demand Market 3 are: $q_{p_5}^1 = 100 - 0.007(t_a^1 + t_i^1 + t_j^1)$, $q_{p_6}^1 = 100 - 0.007(t_d^1 + t_k^1 + t_j^1)$.

We update the supply functions to take into account the exports from Ecuador and Costa Rica to Russia as follows:

$$s_1^1(\pi) = 8,794.81\pi_1^1 + 2,000,000, \quad s_2^1(\pi) = 2,915.59\pi_2^1 + 500,000.$$

Demand functions associated with the paths from Ecuador and Costa Rica to Russia, along with updated demand functions on the previous paths, in tons, are:

$$\tilde{d}_{p_1}^1(\rho, q) = 600,000 - 1,550.95\rho_{p_1}^1 + 21,214.20q_{p_1}^1, \quad \tilde{d}_{p_2}^1(\rho, q) = 300,000 - 642.84\rho_{p_2}^1 + 11,369.22q_{p_2}^1,$$

$$\tilde{d}_{p_3}^1(\rho, q) = 300,000 - 1,419.01\rho_{p_3}^1 + 17,438.79q_{p_3}^1, \quad \tilde{d}_{p_4}^1(\rho, q) = 100,000 - 714.34\rho_{p_4}^1 + 9,617.77q_{p_4}^1,$$

$$\tilde{d}_{p_5}^1(\rho, q) = 600,000 - 1,596.13\rho_{p_5}^1 + 21,717.28q_{p_5}^1, \quad \tilde{d}_{p_6}^1(\rho, q) = 100 - 89.31\rho_{p_6}^1 + 552.42q_{p_6}^1.$$

Finally, the unit cost of transportation associated with the new links and paths, in dollars per ton, are:

$$c_i^1(f, t, T) = 0.00005f_i^1 + 0.2t_i^1 + 25, \quad c_k^1(f, t, T) = 0.00005f_k^1 + 0.2t_k^1 + 20,$$

$$c_j^1(f, t, T) = 0.00002f_j^1 + 0.2t_j^1 + 10,$$

$$\tilde{C}_{p_5}^1(x, T) = c_a^1 + c_i^1 + c_j^1, \quad \tilde{C}_{p_6}^1(x, T) = c_d^1 + c_k^1 + c_j^1.$$

Tables 11 and 12 report, respectively, the equilibrium solution and the function values for Example 5. Table 13 displays the banana trade quality performance measures for Example 5.

Table 11: Computed Equilibrium Values of Paths Flows, Banana Quality, Supply Prices, and Demand Prices for Examples 5 and 6

Computed Equilibrium Values	Example 5	Example 6
$x_{p_1}^{1*}$	1,574,096.84	1,428,165.30
$x_{p_2}^{1*}$	981,068.25	936,088.82
$x_{p_3}^{1*}$	1,158,022.00	976,824.38
$x_{p_4}^{1*}$	641,004.83	582,006.05
$x_{p_5}^{1*}$	1,609,030.06	1,467,533.17
$x_{p_6}^{1*}$	1,301.10	25.52
$q_{p_1}^{1*}$	94.98	91.01
$q_{p_2}^{1*}$	96.73	94.26
$q_{p_3}^{1*}$	96.76	91.76
$q_{p_4}^{1*}$	98.49	95.43
$q_{p_5}^{1*}$	94.83	91.01
$q_{p_6}^{1*}$	96.68	95.09
π_1^{1*}	266.19	212.91
π_2^{1*}	385.30	349.20
$\rho_{p_1}^{1*}$	671.14	710.89
$\rho_{p_2}^{1*}$	651.31	677.60
$\rho_{p_3}^{1*}$	584.46	650.73
$\rho_{p_4}^{1*}$	568.78	610.19
$\rho_{p_5}^{1*}$	658.19	694.83
$\rho_{p_6}^{1*}$	584.61	589.04

The flows of bananas from Ecuador and Costa Rica to Russia, as reported in Table 11, align with real-world data with reference to FAOSTAT(2024), which identifies Russia as one of Ecuador's major importers, at 1.59 million tons in 2022. Russia, however, is a minor destination for Costa Rican bananas with exports of only 1204 tons (Cabezas (2022)). The equilibrium volumes of bananas exported from Ecuador and Costa Rica to the United States (p_3 and p_4) and the European Union (p_1 and p_2) still closely match their values in Example 1 and 3.

The transportation times are calculated as: from Ecuador to the European Union: 716.58 hours, from Costa Rica to the European Union: 466.95 hours, from Ecuador to the United States: 462.81

hours, from Costa Rica to the United States: 214.91 hours, from Ecuador to Russia: 737.59 hours, and from Costa Rica to Russia: 472.89 hours (nearly 30, 19, 19, 9, 31, and 20 days, respectively). In accordance with equation (9), the flow of link a is the sum of flows on all paths passing through it. With Russia added as Demand Market 3, link a (common to paths: p_1, p_3 , and p_5) now carries a total flow of 4.3 million tons, compared to its value in Example 3 of 2.7 million tons. This flow leads to significantly longer transportation times on paths from Ecuador to the European Union and to the United States (p_1, p_3) as compared to Examples 1 and 3. By contrast, paths originating from Costa Rica (p_2, p_4) have transportation times similar to those observed in Examples 1 and 3, as well as to real-world estimates according to Fluentcargo (2024) and Maersk (2024). This is because the newly added Costa Rica - Russia path carries a low flow of only 1,301.10 tons; so it does not alter total flows on the Costa Rica–origin paths. As a result, the congestion-induced delay effects remain negligible for Costa Rica, and the corresponding transportation times stay nearly unchanged. Real-world transportation times from Ecuador to Russia are approximately 30 days, based on Fluentcargo (2024), which, in this example, is higher due to the large flow on link a . Low banana shipments from Costa Rica to Russia result in the lower impact of shipment volume on the link and, hence, shorter transportation time and higher final quality. Real-world data from Fluentcargo (2024) and Searates (2024) report an average transportation time of three to four weeks for shipments from Costa Rica to Russia, indicating that the 20-day outcome for this path agrees reasonably well with actual time, especially given the low flow volumes. In contrast, the longer transportation times on paths: p_1, p_3 , and p_5 contribute to the lower final quality of bananas on those paths as compared to Example 3. This outcome also highlights the essential role of each transportation link in the trade network in reducing times and, thus, in preserving the quality of the bananas that arrive at the demand markets.

Table 12: Function Values at the Equilibrium for Examples 5 and 6

Functions	Example 5	Example 6
s_1^1	4,341,148.90	3,872,522.85
s_2^1	1,623,374.18	1,518,120.39
$\tilde{d}_{p_1}^1$	1,574,096.84	1,428,165.30
$\tilde{d}_{p_2}^1$	981,068.25	936,088.82
$\tilde{d}_{p_3}^1$	1,158,022.00	976,824.38
$\tilde{d}_{p_4}^1$	641,004.83	582,006.05
$\tilde{d}_{p_5}^1$	1,609,030.06	1,467,533.17
$\tilde{d}_{p_6}^1$	1,301.10	25.52
$\tilde{C}_{p_1}^1$	404.95	497.98
$\tilde{C}_{p_2}^1$	266.01	328.40
$\tilde{C}_{p_3}^1$	318.27	437.82
$\tilde{C}_{p_4}^1$	183.48	260.99
$\tilde{C}_{p_5}^1$	392.00	481.92
$\tilde{C}_{p_6}^1$	199.31	239.84

Similar to the decline observed in the equilibrium supply prices for Ecuador and Costa Rica

in Example 3, as compared to Example 1, we observe a decrease in the supply market equilibrium prices: π_1^{1*} and π_2^{1*} in Example 5 as compared to their values in Example 3. However, the equilibrium supply market prices remain reasonably close to the actual price range recorded in the database (FAOSTAT (2024)). On the demand side, the equilibrium demand prices for the bananas on paths from Ecuador to the European Union and the United States ($\rho_{p_1}^{1*}, \rho_{p_3}^{1*}$) increase compared to their values in Example 3. This can be attributed to lower shipment volumes on these routes than in Example 3. Conversely, the demand prices for the bananas on paths from Costa Rica to the European Union and the United States ($\rho_{p_2}^{1*}, \rho_{p_4}^{1*}$) decrease, reflecting the higher shipment volumes exported compared to Example 3. It is important to note that the demand prices on those paths still align closely with the real prices detailed in Examples 1 and 3. Additionally, the demand prices on paths reaching Russia ($\rho_{p_5}^{1*}, \rho_{p_6}^{1*}$) match the actual average import prices in Russia in 2022 of 488 dollars per ton (IndexBox (2024)). Specifically, higher prices are observed for bananas destined for the European Union as compared to those headed to the United States and Russia.

Even with the increased complexity of the banana trade network due to the addition of a demand market, the equilibrium conditions (12) – (14) hold perfectly. As shown in Table 12, Ecuador’s total banana exports exceed 4.34 million tons, combining flows to the European Union, the United States, and Russia. Similarly, Costa Rica exports a total of 1.62 million tons. Due to the longer transportation times from Ecuador to the European Union, the United States, and Russia, the transportation costs for these paths ($\tilde{C}_{p_1}^1, \tilde{C}_{p_3}^1, \tilde{C}_{p_5}^1$) are higher as compared to those originating from Costa Rica ($\tilde{C}_{p_2}^1, \tilde{C}_{p_4}^1, \tilde{C}_{p_6}^1$). It is important to note that the transportation costs for banana volumes exported from Costa Rica to the three demand markets are comparable to the actual quotes given earlier in Section 5 (BR Logistics (2023a,b), FW Freight (2024)).

Regarding the quality performance measures, as presented in Table 13, Ecuador demonstrates higher performance due to significantly larger shipment quantities, as compared to Costa Rica, despite the final quality of the bananas on these paths being noticeably lower than those originating from Costa Rica. Among the demand markets, the European Union exhibits the highest quality measure, followed by the United States and Russia. The network-based performance decreases in Example 5 as compared to Example 3.

Table 13: Banana Quality Trade Performance Measures for Examples 5 and 6

Performance Measures	Example 5	Example 6
$\mathcal{E}_S^{1,1}$	215,442.66	170,937.19
$\mathcal{E}_S^{1,2}$	85,641.01	73,750.44
$\mathcal{E}_D^{1,1}$	184,239.94	156,529.02
$\mathcal{E}_D^{1,2}$	151,358.79	114,386.56
$\mathcal{E}_D^{1,3}$	116,026.77	96,115.86
$\mathcal{E}_{Network}^1$	150,541.84	122,343.81

5.6 Example 6: Example 5 but with Upper Bound Reductions on Maritime Transportation Links via the Panama Canal and Increases in Free-Flow Transportation Times

In Example 6, we explore further the impacts of upper bound reductions on the Panama Canal. For upper bounds on those links passing through the Panama Canal, we set a 40% reduction of their original values similar to what was done for Examples 2 and 4, so that: $u_b = u_e = u_i = 1,800,000$, $u_h = u_f = 1,200,000$, and $u_k = 12,000$ while also increasing the free-flow times of these links to account for additional delays of 500.00 hours. Tables 11, 12, and 13 report the equilibrium solutions, function values, and the banana trade quality performance measures for Example 6, respectively.

As shown in Table 11, and compared to Example 5, the banana flows from Ecuador and Costa Rica to each demand market decrease as follows: on $x_{p_1}^{1*}$: by 9.27%, on $x_{p_2}^{1*}$: by 4.58%, on $x_{p_3}^{1*}$: by 15.64%, on $x_{p_4}^{1*}$: by 9.20%, on $x_{p_5}^{1*}$: by 8.79%, and on $x_{p_6}^{1*}$: by 98.03%. It is interesting to see that the banana exports from Costa Rica to Russia fall to extremely low volumes, only 25.52 tons, after imposing the drought-driven transportation limits. Meanwhile, real data from 2023 (FAOSTAT (2024)) indicates that Costa Rica's banana shipments to Russia amounted to only 196 tons.

The overall transportation times on all Panama-related routes increase substantially, with the time from Ecuador to the European Union now being: 1,284.17 hours, the time from Costa Rica to the European Union: 819.77 hours, the time from Ecuador to the United States: 1,176.78 hours, the time from Costa Rica to the United States: 651.79 hours, the time from Ecuador to Russia: 1,283.71 hours, and the time from Costa Rica to Russia: 700.63 hours (nearly 53, 34, 49, 27, 53, and 29 days, respectively). Although Russia is farther from Costa Rica than the European Union, here, the flow on the Costa Rica–Russia path is exceptionally small (25.52 tons), so congestion effects on this route remain negligible. In contrast, the Costa Rica – European Union path carries a much higher flow (936,088.81 tons), which increases transportation time since its upper bounds are reduced. Consequently, the larger shipment volume to the European Union overshadows the distance factor, resulting in a longer overall transportation time than to Russia. Such prolonged transportation durations clearly erode the final banana quality with paths p_1 and p_5 ending up with the lowest final quality in Example 6. Supply prices for Ecuador and Costa Rica both decline markedly from their values in Example 5, by 20.01% and 9.36%, because fewer bananas are successfully exported. Meanwhile, demand prices increase sharply on all paths with ($\rho_{p_1}^{1*}$ increasing by 5.92%, $\rho_{p_2}^{1*}$ increasing by 4.03%, $\rho_{p_3}^{1*}$ increasing by 11.33%, $\rho_{p_4}^{1*}$ by 7.28%, $\rho_{p_5}^{1*}$ by 5.56%, and $\rho_{p_6}^{1*}$ by 0.75%). The overall transportation times on all routes increase substantially, reaching their highest values compared to all previous examples, as shown in Table 12.

Finally, Table 13 reveals a marked drop in the supply-based, demand-based, and network-based quality measures, consistent with the upper bound reductions and accompanying drought-driven transportation delays. Ecuador continues to achieve higher performance measures than Costa Rica by shipping greater volumes of bananas overall. As for the demand markets, the European Union still enjoys the highest performance measure, largely due to receiving greater banana shipments. This suggests that, in this context, the shipment quantity exerts a greater influence on the quality

performance measure than either the final quality of the bananas or the demand price. In summary, the reduced capacity in the Panama Canal and the longer free-flow times cause the network-based quality metric to fall to its lowest level across all examples, demonstrating how vulnerable the global banana trade can be when key transportation routes face significant transportation limitations.

5.7 Sensitivity Analysis

In this section, we conduct a sensitivity analysis to evaluate the impact of varying upper bounds of maritime links and transportation times on the equilibrium solutions. These analyses are performed using the network configuration of Example 5 and the same data, except for as noted below. In the first two scenarios - Scenarios 1 and 2 - the upper bounds of the maritime transportation links: u_b, u_e, u_f, u_h, u_i , and u_k are reduced by 30% and by 60%, respectively, while maintaining the original free-flow transportation times: $t_b^0 = t_e^0 = 140.00$, $t_f^0 = t_h^0 = 80.00$, and, $t_i^0 = t_k^0 = 200.00$. Scenarios 1 and 2 isolate the effects of upper bounds on the equilibrium solutions. The last two scenarios - Scenarios 3 and 4 - examine the combined effects of reduced upper bounds and increased transportation times. In Scenario 3, the upper bounds of the maritime links: u_b, u_e, u_f, u_h, u_i , and u_k , are reduced by 30%, and the free-flow transportation times: $t_b^1, t_e^1, t_f^1, t_h^1, t_i^1$, and t_k^1 , are increased to 300 hours. Similarly, in Scenario 4, the upper bounds are reduced by 60%, with the free-flow times also set to 300 hours.

Tables 14, 15, and 16 present the equilibrium values for the variables, the functions, and the quality performance measures under the respective scenarios. Figures 5, 6, and 7 illustrate the shipment volumes (log scale), the demand prices, and the quality performance measures across all scenarios.

Observe, from Table 14 and Figure 5, that, in Scenario 1, where the maritime links' upper bounds are reduced by 30% (while free-flow transportation times remain unchanged), there are slight reductions in path flows, final quality, and supply prices as compared to those in Example 5. Demand prices, as presented in Figure 6, show minimal increases due to lower shipments relative to Example 5, suggesting that a moderate upper bound cut does not drastically disturb the trade network. Moving to Scenario 2, path flows and final quality decrease more noticeably, as compared to Scenario 1 and Example 5. Supply prices fall further, notably π_1^{1*} , whereas demand prices rise substantially, especially for the path from Ecuador to Russia ($\rho_{p_5}^{1*}$). Consequently, customers pay higher prices for bananas of lower quality. However, the equilibrium path flow between Costa Rica and Russia increases in Scenarios 1 and 2 as compared to Example 5. Hence, the demand price decreases in Scenarios 1 and 2. Also, a very slight increase is observed in the final quality of bananas exported from Costa Rica to Russia in Scenarios 1 and 2 as compared to results in Example 5.

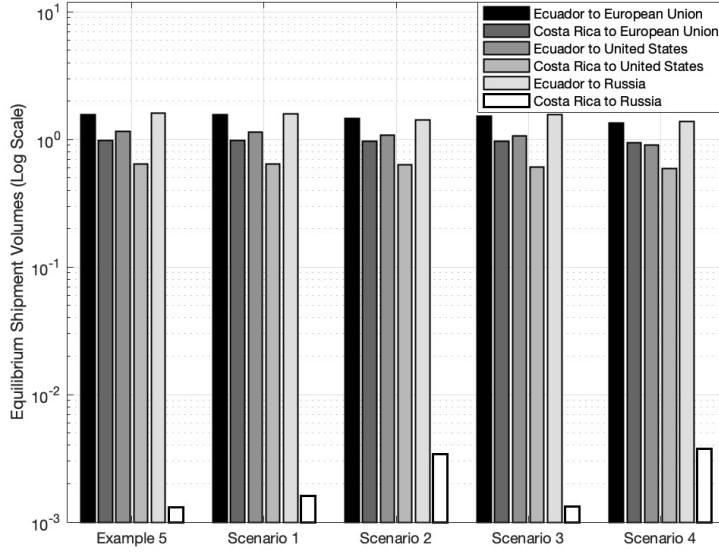


Figure 5: Equilibrium Banana Shipment Volumes in Million Tons under Different Scenarios

Looking at Table 15, in Scenario 1, banana supplies from Ecuador (s_1^1) and Costa Rica (s_2^1) decrease as compared to their values in Example 5. Additionally, demand on all paths declines, as compared to Example 5, except for Costa Rica to Russia, which shows an increase in both Scenarios 1 and 2. Unlike $\tilde{C}_{p_6}^1$, in Scenario 1, transportation costs rise on all paths compared to Example 5. Scenario 2 brings more pronounced decreases in total supplies, especially from Ecuador, whose supply drops to 3.95 million tons. Correspondingly, transportation costs increase notably in Scenario 2, as compared to Example 5 and Scenario 1, except for the path from Costa Rica to Russia.

In Table 16 and Scenario 1, the supply-based and demand-based quality measures show slight reductions from those measures in Example 5, with Ecuador and the European Union keeping the highest quality measures at both the supply and the demand markets. Consequently, the network-based quality measure decreases marginally to 148,258.66. Scenario 2 sees more noticeable drops in supply-based, demand-based, and network-based quality measures, as Figure 7 clearly shows.

Table 14: Computed Equilibrium Values of Paths Flows, Banana Quality, Supply Prices, and Demand Prices under Different Scenarios

Computed Equilibrium Values	Example 5	Scenario 1	Scenario 2	Scenario 3	Scenario 4
$x_{p_1}^{1*}$	1,574,096.84	1,562,106.32	1,457,113.63	1,516,345.73	1,348,751.86
$x_{p_2}^{1*}$	981,068.25	980,399.27	971,567.43	962,845.95	944,380.46
$x_{p_3}^{1*}$	1,158,022.00	1,149,757.70	1,074,266.51	1,065,519.52	906,077.46
$x_{p_4}^{1*}$	641,004.83	640,517.32	635,467.67	610,312.80	592,842.72
$x_{p_5}^{1*}$	1,609,030.06	1,585,673.47	1,426,317.37	1,566,687.11	1,375,898.81
$x_{p_6}^{1*}$	1,301.10	1,614.25	3,427.67	1,333.19	3,756.55
$q_{p_1}^{1*}$	94.98	94.64	91.78	93.38	88.90
$q_{p_2}^{1*}$	96.73	96.69	96.24	95.68	94.69
$q_{p_3}^{1*}$	96.76	96.46	93.91	94.36	89.63
$q_{p_4}^{1*}$	98.49	98.46	98.15	96.95	95.98
$q_{p_5}^{1*}$	94.83	94.31	90.60	93.52	88.73
$q_{p_6}^{1*}$	96.68	96.76	97.13	96.16	96.49
π_1^{1*}	266.19	261.23	222.60	244.30	185.42
π_2^{1*}	385.30	385.01	380.87	368.53	357.03
$\rho_{p_1}^{1*}$	671.14	674.20	702.84	686.56	733.30
$\rho_{p_2}^{1*}$	651.31	651.73	657.50	661.11	672.42
$\rho_{p_3}^{1*}$	584.46	586.60	608.52	620.17	674.45
$\rho_{p_4}^{1*}$	568.78	569.08	571.88	591.01	602.33
$\rho_{p_5}^{1*}$	658.19	665.70	715.09	666.90	721.24
$\rho_{p_6}^{1*}$	584.61	581.60	563.58	581.01	555.89

Table 15: Function Values at the Equilibrium under Different Scenarios

Functions	Example 5	Scenario 1	Scenario 2	Scenario 3	Scenario 4
s_1^1	4,341,148.90	4,297,537.49	3,957,697.51	4,148,552.36	3,630,728.13
s_2^1	1,623,374.18	1,622,530.84	1,610,462.77	1,574,491.94	1,540,979.73
$\tilde{d}_{p_1}^1$	1,574,096.84	1,562,106.32	1,457,113.63	1,516,345.73	1,348,751.86
$\tilde{d}_{p_2}^1$	981,068.25	980,399.27	971,567.43	962,845.95	944,380.46
$\tilde{d}_{p_3}^1$	1,158,022.00	1,149,757.70	1,074,266.51	1,065,519.52	906,077.46
$\tilde{d}_{p_4}^1$	641,004.83	640,517.32	635,467.67	610,312.80	592,842.72
$\tilde{d}_{p_5}^1$	1,609,030.06	1,585,673.47	1,426,317.37	1,566,687.11	1,375,898.81
$\tilde{d}_{p_6}^1$	1,301.10	1,614.25	3,427.67	1,333.19	3,756.55
$\tilde{C}_{p_1}^1$	404.95	412.97	480.24	442.26	547.88
$\tilde{C}_{p_2}^1$	266.01	266.72	276.63	292.58	315.39
$\tilde{C}_{p_3}^1$	318.27	325.37	385.92	375.87	489.03
$\tilde{C}_{p_4}^1$	183.48	184.07	191.01	222.48	245.30
$\tilde{C}_{p_5}^1$	392.00	404.47	492.49	422.60	535.82
$\tilde{C}_{p_6}^1$	199.31	196.59	182.71	212.48	198.86

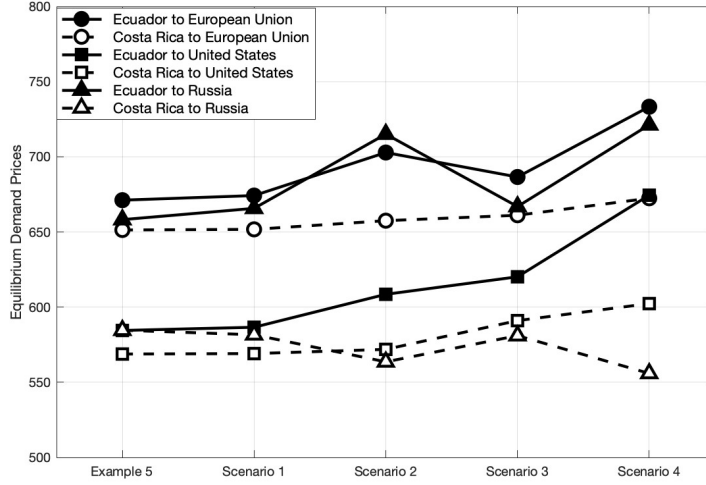


Figure 6: Equilibrium Demand Prices under Different Scenarios

To summarize, reducing the upper bounds on maritime links alone leads to moderate declines in shipment volumes, final quality, and supply prices across the network. As the upper bounds become tighter, these effects become more pronounced, particularly for Ecuador, whose supply shows greater reductions. Meanwhile, demand prices tend to rise in response to lower banana flows, although the route from Costa Rica to Russia can exhibit unexpected increases in shipment volumes, resulting in lower demand prices and slightly higher quality on that path. Overall, these outcomes underscore how upper bounds on maritime links, independent of additional transportation time adjustments, can significantly affect both producers and consumers in the banana trade network.

Table 16: Banana Quality Trade Performance Measures under Different Scenarios

Performance Measures	Example 5	Scenario 1	Scenario 2	Scenario 3	Scenario 4
$\mathcal{E}_S^{1,1}$	215,442.66	210,998.69	178,935.37	196,031.80	151,073.33
$\mathcal{E}_S^{1,2}$	85,641.01	85,518.63	83,957.25	79,898.09	76,039.06
$\mathcal{E}_D^{1,1}$	184,239.94	182,371.08	166,254.40	172,805.91	148,260.28
$\mathcal{E}_D^{1,2}$	151,358.79	149,946.04	137,428.87	131,122.07	107,443.11
$\mathcal{E}_D^{1,3}$	116,026.77	112,458.86	90,655.67	109,966.85	84,965.20
$\mathcal{E}_{Network}^1$	150,541.84	148,258.66	131,446.31	137,964.94	113,556.20

Scenarios 3 and 4 combine upper bound reductions with a free-flow time of 300 hours. Referring to Table 14 and Figure 5, in Scenario 3, all path flows are lower than those in Example 5 and Scenario 1, except $x_{p_6}^{1*}$, which is higher than that in Example 5 and lower than in Scenarios 1 and 2. The transportation times in Scenario 3 increase compared to Example 5 with 944.45 hours for p_1 , 616.80 hours for p_2 , 805.54 hours for p_3 , 434.82 hours for p_4 , 924.70 hours for p_5 , and 547.82 hours for p_6 . Final banana quality shipped on all paths and supply prices decrease compared to

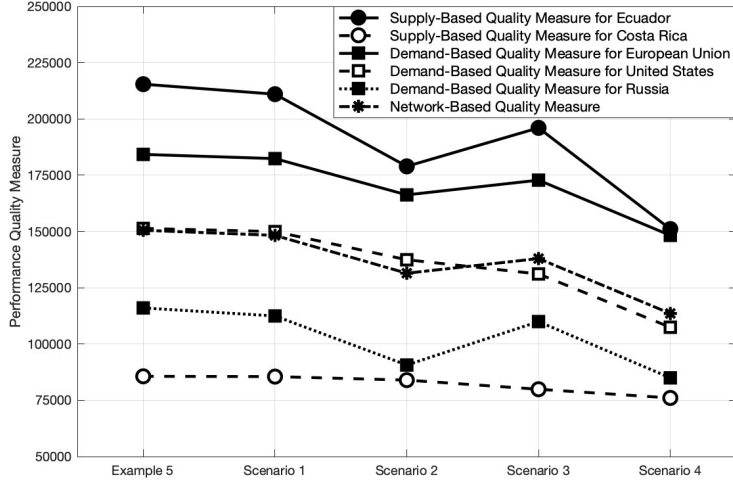


Figure 7: Banana Quality Trade Performance Measures under Different Scenarios

their values in Example 5 and Scenario 1, while demand prices on all paths, except from Costa Rica to Russia, increase from their respective values in Example 5 and Scenario 1. The reductions and increments observed in Scenario 3 relative to Example 5 are more pronounced than those in Scenario 1 relative to Example 5. This highlights the compounded adverse effects of upper bound reductions combined with increased transportation times on the banana trade network.

Scenario 4 exhibits the largest declines in path flows and quality overall, except for $x_{p_6}^{1*}$ and $q_{p_6}^{1*}$, which show an unexpected increase compared to Scenario 3. The transportation times increase compared to Example 5 and Scenario 3 to 1,584.84 hours for p_1 , 757.42 hours for p_2 , 1,480.67 hours for p_3 , 5574.27 hours for p_4 , and 1,609.13 hours for p_5 . Interestingly, the time from Costa Rica to Russia decreases from Scenario 3 to 501.27 hours, which explains the increase in final quality on that path. The supply prices reach their lowest values across all scenarios and Example 5. As in Figure 6, except for $\rho_{p_6}^{1*}$, which decreases due to higher path flows, all demand prices rise, compared to Scenario 3, with a more noticeable increase in prices of Ecuador’s bananas to three demand markets. Scenario 4 underscores how tight upper bounds and prolonged transportation times significantly impact both equilibrium flows and prices across the network.

Observe from Table 15 that, in Scenario 3, when increasing the time alongside upper bound reductions, supplies at both supply markets and demand on all paths decline compared to Example 5 and Scenario 1. Transportation costs rise more than in Scenario 1 and Example 5, highlighting the compounded effect of reduced upper bounds and slower transportation times. Finally, Scenario 4 intensifies these trends: Ecuador and Costa Rica supplies decline to 3.63 and 1.54 million tons, respectively, while flows on the paths shrink substantially, except for $\tilde{d}_{p_6}^1$, which increases compared to Example 5 and Scenario 3. The highest transportation costs are observed on all paths in Scenario 4 among all scenarios. It is noteworthy that the transportation cost for trade between Costa Rica

and Russia in Scenario 4 is lower than in Scenario 3 but higher than in Example 5 and Scenarios 1 and 2.

The impact of adjustment in Scenarios 3 and 4 on quality measures is illustrated in Table 16 and Figure 7. In Scenario 3, all quality performance measures decline from their values in Example 5 and Scenario 1. Scenario 4 further amplifies these reductions, yielding the lowest overall quality results observed in the supply and demand markets, as well as the trade network. In Scenario 4, the Costa Rica-Russia path p_6 sees an increase in shipments, higher final quality, and a lower demand price relative to Scenario 3. However, Costa Rica’s other two routes, Costa Rica-European Union path p_2 and Costa Rica-United States path p_4 , handle much larger volumes, each exhibiting notable declines in shipment and quality, along with rising demand prices. Consequently, while $x_{p_6}^{1*}$, $q_{p_6}^{1*}$, $\rho_{p_6}^{1*}$ individually improve, their minor share of Costa Rica’s total exports cannot offset the significant deterioration on paths p_2 and p_4 . Hence, Costa Rica’s overall supply-based quality measure still declines in Scenario 4. These findings highlight how prolonged transportation times, combined with tighter upper bounds, substantially diminish the trade network’s ability to export high volumes of high-quality bananas at mutually beneficial prices for producers and consumers.

6. Summary and Conclusions

In this paper, we constructed a commodity trade network equilibrium model for fresh produce that explicitly incorporates quality deterioration across multi-link transportation routes. By allowing routes to consist of multiple links, each of which could represent a distinct transportation mode (e.g., maritime, rail, or truck), we capture complex and real shipment routes in which capacity reductions and bottlenecks may occur on any link. We further introduced nonlinear time delay functions dependent on both the total flow on a link and its upper bound, adapted from the Bureau of Public Roads (BPR) formulation. In contrast to prior linear approaches, that also focused on paths of single links, this model enables flow-dependent transportation times that simultaneously account for all commodities sharing a link. Through these features, our framework reflects how reduced or enhanced upper bounds on each link can significantly influence both transportation times and the quality of the fresh produce.

The governing equilibrium conditions of the fresh produce trade network were presented and formulated as a variational inequality problem. In addition, we proposed commodity quality trade network performance measures — supply-based, demand-based, and network-based metrics — that allow decision-makers to assess quality levels from multiple perspectives. These measures can be applied to a single commodity or aggregated across all commodities, enabling focused or broader evaluations of trade network performance.

We demonstrated the practical applicability of our model through numerical examples focusing on banana shipments from Ecuador and Costa Rica to the European Union, the United States, and Russia. Bananas are a very popular fruit with nutritional value. The examples incorporate drought-induced congestion in the Panama Canal, illustrating how upper bound reductions and extended free-flow transportation times translate into increased transportation times, lowered shipment vol-

umes, and deteriorated final fresh produce quality. Comparisons of our new model with nonlinear congestion on transportation links with linear congestion and free-flow transportation (uncongested links) reveal that, while the linear and no-congestion cases provide useful benchmarks, they do not account for endogenous link upper bounds or congestion effects that are common on heavily used trade routes. In contrast, our model with nonlinear transportation delay link functions provides a more realistic representation, since transportation times, commodity supply market and demand market prices, and commodity quality levels adjust accordingly in response to commodity shipment volumes.

Our outcomes align closely with real-world data on banana shipments, prices, and transportation costs, underscoring the model’s ability to capture important trade-offs among banana shipment volumes, prices, and quality. We also conducted a sensitivity analysis to explore the relative impacts of upper bound reductions alone as well as upper bound reductions combined with longer transportation times. The results revealed that both factors substantially affect fresh produce commodity equilibrium flows, prices, and final quality measures, with the most pronounced effects arising from compounded disruptions in terms of capacity and transportation times.

From a policy and managerial standpoint, our findings emphasize the vulnerability of perishable commodities when critical transit routes face disruptions. Monitoring flow-dependent times and quality deterioration across individual links can be critical for supply chain planners looking to mitigate risks and to maintain fresh produce quality. Identifying vulnerable transportation links is critical for understanding risk in perishable trade networks. In our framework, however, vulnerability is not introduced as a separate exogenous concept or metric, but rather emerges endogenously through the equilibrium outcomes already reported in the numerical study.

Specifically, in our model, a link is vulnerable if small changes in capacity or flow lead to disproportionately large impacts on transportation time, commodity quality, equilibrium shipments, and/or prices. These mechanisms are explicitly embedded in the nonlinear congestion (time-delay) functions and quality deterioration expressions. As a result, vulnerable links can be directly identified from the reported numerical examples by examining links that (i) operate close to their upper bounds, (ii) experience nonlinear congestion effects, and (iii) drive significant quality and flow reductions under parameter changes.

The benchmark comparisons in Section 5 (Examples 1–2) yield a clear takeaway: when equilibrium flows operate sufficiently below link upper bounds, the nonlinear, linear, and no-congestion specifications lead to broadly similar implications for link importance. However, under upper bound tightening, when utilization rises to moderate-to-high levels (e.g., approximately 76–78% of upper bounds in Example 2), link rankings become more sensitive to the congestion specification because travel time penalties and, hence, quality deterioration diverge across formulations. Accordingly, protection should be prioritized for links that enter this high-utilization range, since the linear specification can impose disproportionately large travel time penalties already at moderately utilized links, while the nonlinear specification more sharply emphasizes the highest-utilization maritime link.

Our numerical study clearly highlights that the maritime links through the Panama Canal are the most vulnerable links in the trade networks, of increasing complexity, that we examined. These links, when characterized by long free-flow transportation times and reduced upper bounds, as affected by drought-induced capacity reductions, lead to nonlinear increases in transportation time, accelerated quality deterioration, reduced equilibrium shipments, and shifts in prices at both supply and demand markets. These effects are consistently observed across the baseline and congestion specification variants presented in the paper.

In addition, the numerical examples reveal secondary vulnerability effects on downstream links that aggregate flows from multiple paths. These links become stressed not because of their own intrinsic characteristics alone, but due to spillover effects from upstream congestion and rerouting behavior, further reinforcing how vulnerability emerges endogenously from the network structure, function characteristics, bounds, and the resulting equilibrium flows.

Furthermore, by employing the proposed quality performance measures, decision-makers can discern which supply and demand markets excel in maintaining fresh produce quality while also estimating the trade network's overall quality performance.

Several directions are worth investigating in future research. Beyond the Panama Canal, the Suez Canal is another vital canal, particularly for trade between Europe and Asia, that is experiencing disruptions. Hence, expanding the set of transportation routes would be worthwhile. It would be interesting to extend the model to include aspects of uncertainty and to apply the extension to Suez-based trade, which might uncover how capacity reductions (e.g., from Houthi attacks in the Red Sea) influence perishable commodity flows, transportation times, and final quality. Also, additional commodity types could be included into numerical example studies to explore competition for shared links in even more complex networks. Plus, including various policy instruments, such as tariffs, which may result in both production location changes and also use of different transportation routes, might be enlightening; the same for explicit inclusion of exchange rates. We leave such research for the future.

Acknowledgments

The authors thank the Editor and the two anonymous reviewers for their constructive comments and suggestions on three earlier versions of this paper.

Declaration of Competing Interest None.

References

Arrhenius, S. (1889). Über die reaktionsgeschwindigkeit bei der inversion von rohrzucker durch sauren. *Z. für Phys. Chem.*, 4, 226-248.

Banana Link (2024). All about bananas and why bananas matter. Retrieved from <https://www.bananalink.org.uk/all-about-bananas/>. Accessed January 1, 2025.

Besik, D., & Nagurney, A. (2017). Quality in competitive fresh produce supply chains with application to farmers' markets. *Socio-Economic Planning Sciences*, 60, 62-76.

Besik, D., & Nagurney, A. (2025). Multicommodity fresh produce trade networks with quality deterioration under congestion and transportation capacities. *Journal of Global Optimization*. Available at: <https://link.springer.com/article/10.1007/s10898-025-01507-3>

Besik, D., Nagurney, A., & Dutta, P. (2023). An integrated multitiered supply chain network model of competing agricultural firms and processing firms: The case of fresh produce and quality. *European Journal of Operational Research*, 307(1), 364-381.

Birge, J., Chan, T., Pavlin, M., & Zhu, I.Y. (2022). Spatial price integration in commodity markets with capacitated transportation networks. *Operations Research*, 70(3), 1739-1761.

BR Logistics (2023a). Ship a container to Ecuador. Retrieved from <https://www.brlogistics.net/us/ship-a-container/to-ecuador/>. Accessed November 22, 2024.

BR Logistics (2023b). Ship a container to Costa Rica. Retrieved from <https://www.brlogistics.net/us/ship-a-container/to-costa-rica/>. Accessed November 22, 2024.

Cabezas, G. (2022). Russia-Ukraine conflict affecting the Ecuadorian banana industry. Retrieved from <https://www.tridge.com/stories/russia-ukraine-conflict-affecting-the-ecuadorian-banana-industry>. Accessed December 30, 2024.

Dafermos, S., & Nagurney, A. (1984). Sensitivity analysis for the general spatial economic equilibrium problem. *Operations Research*, 32, 1069-1086.

de Keizer, M., Akkerman, R., Grunow, M., Bloemhof, J. M., Haijema, R., & van der Vorst, J. G. (2017). Logistics network design for perishable products with heterogeneous quality decay. *European Journal of Operational Research*, 262(2), 535-549.

FAOSTAT (2022). Crops and livestock products. Retrieved from <https://www.fao.org/faostat/en/#data/QCL>. Accessed September 14, 2024.

FAOSTAT (2024). Bananas: Production, trade and producer's price data. Retrieved from <http://www.fao.org/faostat/en/#data>. Accessed September 14, 2024.

Florian, M., & Los, M. (1982). A new look at static spatial price equilibrium models. *Regional Science and Urban Economics*, 12, 579-597.

Fluentcargo (2024). Plan your next shipment route with all the available information. Retrieved from <https://www.fluentcargo.com/search>. Accessed January 1, 2025.

Food and Agriculture Organization of the United Nations (2021). Banana market review 2021. Retrieved from <https://www.fao.org/documents/card/en/c/CC1610EN/>. Accessed November 20, 2024.

Food and Agriculture Organization of the United Nations (2023). Banana market review 2022.

Retrieved from <https://www.fao.org/3/cc6952en/cc6952en.pdf>. Accessed October 7, 2024.

Food and Agriculture Organization of the United Nations (2025). Markets and trade. Retrieved from <https://www.fao.org/markets-and-trade/commodities-overview/bananas-tropical-fruits/bananas/en#:~:text=Banana%20export%20earnings%20help%20to,household%20income%20of%20smallholder%20farmers..> Accessed January 6, 2025.

FreshPlaza (2025). Ecuador's banana industry closely watching Panama Canal delays. Retrieved from <https://www.freshplaza.com/north-america/article/9577012/ecuador-s-banana-industry-closely> Accessed January 4, 2025.

FreshFruitPortal.com (2024). Ecuador sees banana production dip, lower sales to EU on higher minimum price. Retrieved from <https://www.freshfruitportal.com/news/2024/06/28/ecuadorian-banana-prod> Accessed September 14, 2024.

FWFreight (2024). International container quotes. Retrieved from <https://fwfreight.com>. Accessed October 26, 2024.

Glauser, Y.M. (2021). Maritime Transportation: Between AVs and Tankers, There is (Not) the Middle of the Sea. Master's thesis, ETH, Zurich, Switzerland.

Hassani, D., Nagurney, A., Nivievskiy, O., & Martyshev, P. (2025). A multiperiod multicommodity capacitated international agricultural trade network equilibrium model with applications to Ukraine in wartime. *Transportation Science*, 59(1), 143-164.

IndexBox (2024). Russian Federation – bananas: Market analysis, forecast, size, trends and insights. Retrieved from <https://www.indexbox.io/search/banana-price-russia/#price-forecast>. Accessed November 3, 2024.

International Fresh Produce Association (2023). State of the industry report. Retrieved from <https://www.pma.com/siteassets/files/soi/2023-soi-report.pdf>. Accessed January 1, 2026.

International Transport Forum (2016). Capacity to grow: Transport infrastructure needs for future trade growth. Paris, France.

Joshi, R. (2022). 7 major ports in Costa Rica. Retrieved from <https://www.marineinsight.com/know-more/ports-in-costa-rica/>. Accessed October 26, 2024.

Karst, T. (2024). Banana imports rise in volume and value. Retrieved from <https://www.thepacker.com/news/produce-crops/banana-imports-rise-volume-and-value>. Accessed October 26, 2024.

Kim, Y.G., & Mahmassani, H.S. (1987). Link performance functions for urban freeways with asymmetric car - truck interactions. *Transportation Research Record*, 1120, 32-39.

Korpelevich, G.M. (1977). The extragradient method for finding saddle points and other problems.

Matekon, 13, 35–49.

Labuza, T.P. (1984). Application of chemical kinetics to deterioration of foods. *Journal of Chemical Education*, 61(4), 348-358.

Lin, M. (2025). Factbox: Red Sea transits in renewed focus following Houthis' first attacks in 2025. Retrieved from <https://www.spglobal.com/commodity-insights/en/news-research/latest-news/shipping/070925-factbox-red-sea-transits-in-renewed-focus-following-houthis-first>. Accessed January 1, 2026.

Liu, J., Wang, X., & Chen, J. (2023). Port congestion under the COVID-19 pandemic: The simulation-based countermeasures. *Computers & Industrial Engineering*, 183, 109474.

Maersk (2024). Schedules. Retrieved from <https://www.maersk.com/schedules/pointToPoint>. Accessed January 1, 2025.

Marco, A., (2023). Watermelon: Storage, transport and preservation. Retrieved from <https://antoniomarco.com/news/en/watermelon-storage-transport-and-preservation/>. Accessed January 3, 2026

Millard, C. (2019). From farm to table. U.S. Department of Transportation. Federal Highway Administration. Publication Number: FHWA-HRT-19-004.

Nagurney, A. (1999). *Network Economics: A Variational Inequality Approach*, second and revised edition. Kluwer Academic Publishers, Dordrecht, The Netherlands.

Nagurney, A., & Aronson, J. (1989). A general dynamic spatial price network equilibrium model with gains and losses. *Networks*, 19(7), 751-769.

Nagurney, A., & Besik, D. (2022). Spatial price equilibrium networks with flow-dependent arc multipliers. *Optimization Letters*, 16, 2483–2500.

Nagurney, A., Hassani, D., Nivievskiy, O., & Martyshev, P. (2023). Exchange rates and multicommodity international trade: Insights from spatial price equilibrium modeling with policy instruments via variational inequalities. *Journal of Global Optimization*, 87, 1-30.

Nagurney, A., Hassani, D., Nivievskiy, O., & Martyshev, P. (2024a). Multicommodity international agricultural trade network equilibrium: Competition for limited production and transportation capacity under disaster scenarios with implications for food security. *European Journal of Operational Research*, 314(1), 1127-1142.

Nagurney, A., Hassani, D., Nivievskiy, O., & Martyshev, P. (2024b). Quantification of international trade network performance under disruptions to supply, transportation, and demand capacity, and exchange rates in disasters. In: *Dynamics of Disasters - From Natural Phenomena to Human Activity*, I.S. Kotsireas, A. Nagurney, P.M. Pardalos, S. Pickl, and C. Vogiatzis, Editors, Springer Nature Switzerland AG, pp 151-179.

Nagurney, A., & Qiang, Q. (2009). *Fragile Networks: Identifying Vulnerabilities and Synergies in an Uncertain World*. Edward Elgar Publishing, Cheltenham, England.

O'Dell, H. (2024). From oil to Ikea furniture: Red Sea conflict and Panama Canal drought delay shipments and could increase emissions. Retrieved from <https://globalaffairs.org/commentary/blogs/oil-ikea-furniture-red-sea-conflict-and-panama-canal-drought-delay-shipments>. Accessed January 3, 2025.

Port Economics, Management and Policy (2022). The transport and handling of bananas. Retrieved from <https://porteconomicsmanagement.org/pemp/contents/part5/bulk-breakbulk-terminal-design-equivalent-handling-bananas/>. Accessed January 1, 2025.

Portfolio (2015). Going bananas: A journey from Ecuador to the Port of New York and New Jersey. Retrieved from <https://portfolio.panynj.gov/2015/04/30/going-bananas-a-journey-from-ecuador-to-ny>. Accessed January 1, 2025.

ProducePay (2023). Drought impact on Panama Canal transit and agricultural trade. Retrieved from <https://producepay.com/resources/drought-impact-on-panama-canal-transit-and-agricultural-trade/>. Accessed January 4, 2025.

Ramirez, S. (2023). Panama Canal drought causes slot reductions and extended shipping delays. Retrieved from <https://www.freshfruitportal.com/news/2023/12/04/panama-canal-drought-causes-slot-reductions-and-extended-shipments/>. Accessed January 1, 2026.

Research and Markets (2019). Global banana market 2019–2024: Increasing health consciousness driving the banana market. Retrieved from <https://www.prnewswire.com/news-releases/global-banana-market-2019-2024-increasing-health-consciousness-driving-the-banana-market-300848111.html>. Accessed December 22, 2024.

Ruiz, S., Shintani, Ch. (2024). Drought in Panama is disrupting global shipping: These 7 graphics show how. Retrieved from <https://www.woodwellclimate.org/drought-panama-canal-7-graphics/>. Accessed December 30, 2024.

Samuelson, P.A. (1952). Spatial price equilibrium and linear programming. *American Economic Review*, 42, 283-303.

Sanders, F.M., Verhaeghe, R.J., & Dekker, S. (2007). Investment dynamics for a congested transport network with competition: Application to port planning. *The Proceedings of the 23th International Conference of The System Dynamics Society*, 17-21.

Searates (2024). Find the best freight quote. Retrieved from <https://www.searates.com/distance-time/>. Accessed September 16, 2024.

Special Report 209: Highway Capacity Manual (1985). TRB, National Research Council, Washington, DC.

Takayama, T., & Judge, G.G. (1964). Spatial equilibrium and quadratic programming. *Journal of*

Farm Economics, 46(1), 67-93.

Takayama, T., & Judge, G.G. (1971). Spatial and Temporal Price and Allocation Models. North-Holland Publishing Company, Amsterdam, The Netherlands.

Taoukis, P.S., & Labuza, T.P. (1989). Applicability of time-temperature indicators as shelf life monitors of food products. *Journal of Food Science*, 54(4), 783-787.

Thore, S. (1986). Generalized network spatial equilibrium: The deterministic and the chance-constrained case. *Papers in Regional Science*, 59(1), 93-102.

Tijskens, L.M.M., & Polderdijk, J.J. (1996). A generic model for keeping quality of vegetable produce during storage and distribution. *Agricultural Systems*, 51(4), 431-452.

Tomorrow's Affairs (2023). No immediate solution to the Panama Canal's bottleneck – a disruption affecting global trade. Retrieved from <https://tomorrowsaffairs.com/no-immediate-solution-to-the-panama-canal-bottleneck/>. Accessed January 3, 2025.

Traffic Assignment Manual (1964). Bureau of Public Roads, U.S. Department of Commerce.

Tridge (2024). Congestion in the Panama Canal affects Ecuador's banana exports. Retrieved from <https://www.tridge.com/news/congestion-in-the-panama-canal-affects-banan-cqtkgw>. Accessed January 4, 2024.

UN Comtrade Database (2022). International trade statistics. Retrieved from <https://comtrade.un.org/data/>. Accessed November 20, 2024

United States Department of Agriculture Foreign Agricultural Service (2024). Red Sea disruptions challenge Egyptian citrus exports. Report EG2024-0005, March 13.

U.S. Energy Information Administration (2023). Drought at the Panama Canal delays energy shipments, increasing shipping costs. Retrieved from <https://www.eia.gov/todayinenergy/detail.php?id=60842>. Accessed January 3, 2025.

Yamada, T., Russ, B.F., Castro, J., & Taniguchi, E. (2009). Designing multimodal freight transport networks: A heuristic approach and applications. *Transportation Science*, 43(2), 129-143.

Yan, Y. (2016). Sensitivity Analysis of Imported Container Volumes to Surcharge Fees via a User-Equilibrium Model. Master's thesis, Cornell University, Ithaca, New York.

Yan, Z., Sousa-Gallagher, M.J., & Oliveira, F.A. (2008). Mathematical modelling of the kinetic of quality deterioration of intermediate moisture content banana during storage. *Journal of Food Engineering*, 84(3), 359-367.

Yu, M., & Nagurney, A. (2013). Competitive food supply chain networks with application to fresh produce. *European Journal of Operational Research*, 224(2), 273-282.